1960

Reduction of wind-generated antenna tracking error through conditional feedback compensation

Hart, Richard L.; Hostettler, Stephen J.

Monterey, California: U.S. Naval Postgraduate School

REDUCTION OF WIND-GENERATED ANTENNA TRACKING ERROR THROUGH CONDITIONAL FEEDBACK COMPENSATION

RICHARD L. HART
and
STEPHEN J. HOSTETTLER

REDUCTION OF WIND-GENERATED ANTENNA TRACKING ERROR THROUGH CONDITIONAL FEEDBACK COMPENSATION

* * * * *

Richard L. Hart

and

Stephen J. Hostettler

REDUCTION OF WIND-GENERATED ANTENNA TRACKING ERROR THROUGH CONDITIONAL FEEDBACK COMPENSATION

by

Richard L. Hart
Lieutenant, United States Navy

and

Stephen J. Hostettler
Lieutenant, United States Navy

Submitted in partial fulfillment of
the requirements for the degree of

MASTER OF SCIENCE
IN
ELECTRICAL ENGINEERING

United States Naval Postgraduate School
Monterey, California

1 9 6 0

REDUCTION OF WIND-GENERATED ANTENNA TRACKING ERROR THROUGH CONDITIONAL FEEDBACK COMPENSATION

by

Richard L. Hart

and

Stephen J. Hostettler

This work is accepted as fulfilling
the thesis requirements for the degree of
MASTER OF SCIENCE
IN
ELECTRICAL ENGINEERING
from the
United States Naval Postgraduate School

ABSTRACT

The advent of the missile and satellite era has brought with it the need for large and highly accurate radar tracking systems. Thus, the antenna tracking error generated by wind disturbances has become a significant consideration. This study presents a compensation technique which substantially reduces these disturbance errors without degradation of the system response to the tracking input.

The study was proposed by Philco Corporation, Western Development Laboratories, Palo Alto, California. The proposal resulted from tests conducted on a production model of a satellite tracking system having a 60 foot, solid skin, high inertia antenna. A large portion of this thesis was accomplished at the Philco Laboratories during the Summer of 1960.

The authors wish to express their appreciation to Dr. M. P. Pastel of the U. S. Naval Postgraduate School for his assistance and counsel in the preparation of this thesis and to Mr. L. J. Harvey of Philco Corporation for his assistance in the development of the problem and for the generous facilities made available to the authors.

TABLE OF CONTENTS

Section	TITLE	Page
1.	Introduction	1
2.	Development of the Basic Approach	4
3.	Development of Basic System	7
4.	Analysis of Basic System	15
5.	Development of Compensation Technique	29
6.	Determination of Conditional Feedback Compensator	41
7.	Selection of Disturbance Input	50
8.	Evaluation of the Conditional Feedback Compensation	55
9.	Conclusions	63
10.	Bibliography	65

LIST OF ILLUSTRATIONS

Figure		Page
2-1.	Block Diagram of a Conventional Control System	4
2-2.	Basic Conditional Feedback Control System	5
3-1.	Block Diagram of Hydraulic Drive System	7
3-2.	Block Diagram of Hydraulic System with Synthesized Loading	8
3-3.	Block Diagram of Initial Basic System	13
4-1.	Nyquist Plot for Initial Basic System	16
4-2.	Bode Diagram for Initial Basic System	17
4-3.	Bode Diagram for Initial Basic System with Added Complex Zero Compensator	21
4-4.	Block Diagram of Basic System with Complex Zero Compensator and Gain Modifications	25
4-5.	Transient Response of Basic System to Unit Step Disturbance Input (U)	26
4-6.	Disturbance-Output Frequency Response of Basic System	27
5-1.	Block Diagram of Proposed Conditional Feedback System	29
5-2.	Representing Function Pole and Zero Placement	36
6-1.	System Responses to Unit Step Disturbances	42
6-2.	Root Locus of Complex Roots of Representing Function	44
6-3.	Measurement of Phase Difference (γ)	46
7-1.	Representative Wind Velocity Profile	51
7-2.	Wind Moment Coefficient vs. Angle of Wind Incidence	53

Figure		Page
8-1.	System Responses to a Step Velocity Disturbance Input	56
8-2a.	Wind Gust Disturbance Response (.5 sec. interval)	57
8-2b.	Wind Gust Disturbance Response (.25 sec. interval)	59
8-2c.	Wind Gust Disturbance Response (1.0 sec. interval)	60
8-3.	Disturbance-Output Frequency Response of Compensated System	61
I-1.	Complex Zero Compensator Schematic	66
II-1.	Pole and Zero Plot of $1/1+F_o$ u(t) for Determination of Residue at Pole (-1.74)	70
II-2.	Pole and Zero Plot of $1/1+F_o$ u(t) for Determination of Residue at Pole (-22.63 + j14.55)	72
III-1.	Block Diagram of Final Hydraulic System	77
IV-1.	Block Diagram of System with Conditional Feedback and R=O	79
IV-2.	Analog Simulation of the Conditional Feedback System for Disturbance Response	83

1. Introduction

The purpose of this study is to present a compensation technique for reducing antenna tracking errors caused by wind-gust disturbances. The antenna system upon which this study is based is the position control system for a 60 foot radar antenna. This system meets the desired response to the tracking input. However, the tracking error caused by wind gusting is not acceptable. The compensation utilized must reduce this error without affecting the system response to the tracking input. This problem corresponds to having an antenna system installed at the tracking site which meets the designed input tracking response. Data showed excessive tracking error resulting from dynamic wind pressure on the solid skin of the large, high inertia dish. This error must be reduced by adding some type of compensation that will not modify the designed tracking input response.

An error of a few seconds of arc can be excessive in determining the precise position of a high altitude orbiting satellite. To meet such stringent error regulating requirements while, at the same time, achieving acceptable tracking input response using conventional compensation techniques poses a formidable problem. Compensating techniques require the sensing of the effects of the wind loading on the antenna system. Wind sensing might take the form of external devices such as sensitive annamometers. These might be placed in locations around the periphery of the antenna and at distances so as to determine in advance the load disturbance which the

antenna would see. Although the nature of a prediction sensing device lends itself to the development of the ideal regulation system, the accuracy of the prediction must of necessity be at least as accurate as the tolerance of the desired output response. To date, no wind sensing transducers have been produced that measure accurately transient wind conditions over a sufficiently small increment of time. Even if such devices were feasible and available, their sensing would not necessarily reflect the actual loading of the antenna dish some distance away. A mountainous site might be expected to show large drafting and eddy-currents about the dish which would preclude the accuracy of any external sensing device to determine actual dish loading.

A second and more reasonable approach might take the form of a sampling of the torque on the antenna drive shaft. Corrections would then be made in the control system based upon these samplings. This approach is complicated and expensive, and at least part time use of a digital computer would be required.

A simpler and more direct approach would be to continuously compare the output position under external loading with the output obtained having no external load with the same tracking input. The difference of these outputs would then be a measure of the effects of transient wind loading on the antenna. Although this approach in no way predicts the loading effect, it does permit the accurate measurement of the effect which in turn may be compensated at a faster rate than that possible by the basic system.

The solution presented here will be developed in the above manner using as the basic approach the conditional feedback concept set forth in the American Institute of Electrical Engineers' publication, "Applications and Industry," July 1955, by G. Lang and J. M. Ham. The conditional feedback system permits design specifications on input-output response and on disturbance-output response to be met independently.

To prevent repetition and to simplify the presentation, only the azimuth axis of rotation will be considered. Design criteria for the compensation will be developed based on selected arbitrary requirements for disturbance-output response improvement. A specific compensation will be designed using the developed criteria and the response will be determined for various disturbance inputs. A design technique is developed which facilitates the determination of this compensation.

An investigation of the characteristics of a severe wind gust disturbance will be utilized to develop a disturbance input which will subject the compensated system to the most demanding conditions expected.

An analog computer simulation will be made of the complete compensated system. Data will be displayed showing the effects of the selected compensation for various wind disturbance inputs.

2. Development of the basic approach.

In the conventional single-loop feedback control system the input-output response, as well as the disturbance-output response, are dependent on the feedback. Thus, in most cases utilizing conventional feedback control, a compromise of the input response must be accepted if a satisfactory disturbance response is to be achieved. Fig. 2-1 shows such a conventional control system.

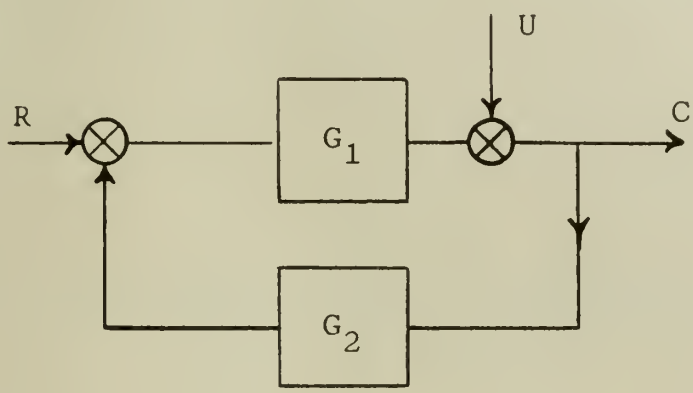

Figure 2-1. Diagram of conventional control system.

In Fig. 2-1, G_1 is the Laplace transform of some control system; G_2 represents the feedback compensation. R is the normal input signal to the system; U is the disturbance signal at the output of the system; C is the final system output. The transfer functions associated with Fig. 2-1 are readily developed as follows:

$$C = G_1(R - G_2C) + U$$

$$C(1 + G_1G_2) = G_1R + U$$

$$C = \frac{G_1}{1 + G_1G_2} R + \frac{1}{1 + G_1G_2} U \qquad (2\text{-}1)$$

Thus, the feedback G_2 affects both input and disturbance

responses. However, the problem treated in this thesis is one in which the effects of disturbance must be compensated without compromise of the given input-output response. A compensation technique meeting these requirements has been presented in "Conditional Feedback Systems" by G. Lang and J. M. Ham [1] and will be used as the basis for the approach of this thesis problem.

A basic configuration for a linear conditional feedback system is shown in Fig. 2-2, where G_1, G_2, R, U, C, are defined as in Fig. 2-1.

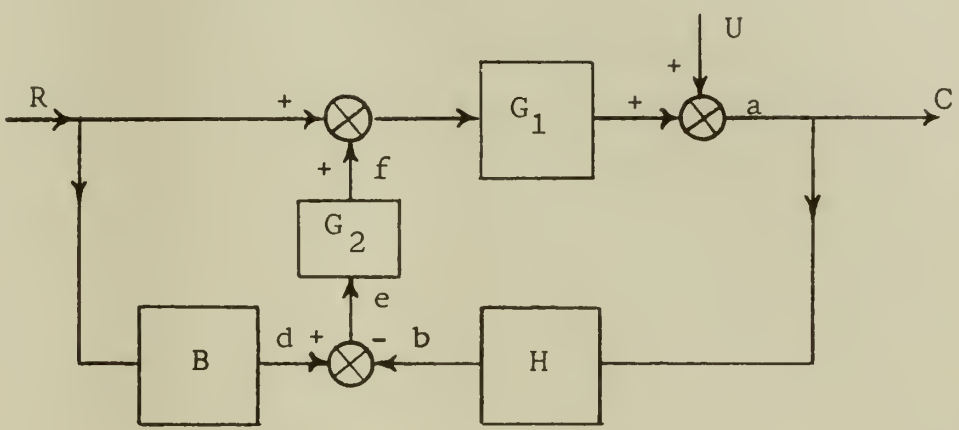

Figure 2-2. Basic conditional feedback control system.

The output C of Fig. 2-2 is

$$C = \frac{G_1(1 + BG_2)}{1 + G_1G_2H} R + \frac{1}{1 + G_1G_2H} U. \qquad (2\text{-}2)$$

Let B in equation (2-2) be defined as

$$B = G_1H. \qquad (2\text{-}3)$$

Equation (2-2) then becomes

$$C = G_1R + \frac{1}{1 + G_1G_2H} U. \qquad (2\text{-}4)$$

Letting U and R be alternately zero,

$$\left(\frac{C}{R}\right)_{U=0} = G_1 \ , \tag{2-5}$$

and

$$\left(\frac{C}{U}\right)_{R=0} = \frac{1}{1 + G_1G_2H} \ . \tag{2-6}$$

Equation (2-5) shows that, when B is defined by equation (2-3), the input response is dependent only on G_1. Thus, G_2H can be utilized to modify the disturbance response without affecting the input response. The output sensing device would normally be described by H. If it is assumed that H = 1, then B becomes equal to G_1 (equation (2-3)). The purpose of the function B is shown by considering the system operation in Fig. 2-2. The feedback signal (b) is equal to (a) since H = 1. With B defined as equal to G_1, (d) is equal to (a) with U equal to zero. Thus, the difference signal (e) is equal to zero and no compensation signal is developed. Clearly, (d) is equivalent to the desired output response and thus B is called a "reference model." The reference model is an undisturbed representation of the transfer characteristics of the antenna drive system. This conditional feedback approach permits the use of the feedback function G_2 to accomplish the desired disturbance compensation without change to the original input response.

3. Development of basic system.

The basic system investigated in this thesis represents the azimuth axis position control system of an actual land-based tracking radar having a sixty foot diameter antenna. The system consists of a hydraulic drive with tachometer feedback and suitable reduction gearing, together with cascaded electronic compensation and position feedback loop.

Prior to any possible investigation of the basic system, the hydraulic drive system transfer functions had to be derived. This hydraulic system consisted of a servo control value and amplifier, a D. C. motor-driven constant displacement pump and associated hydraulic drive motor, and reduction gearing. The hydraulic system was enclosed with a tachometer feedback loop.

The block diagram of this hydraulic drive system is shown in Fig. 3-1.

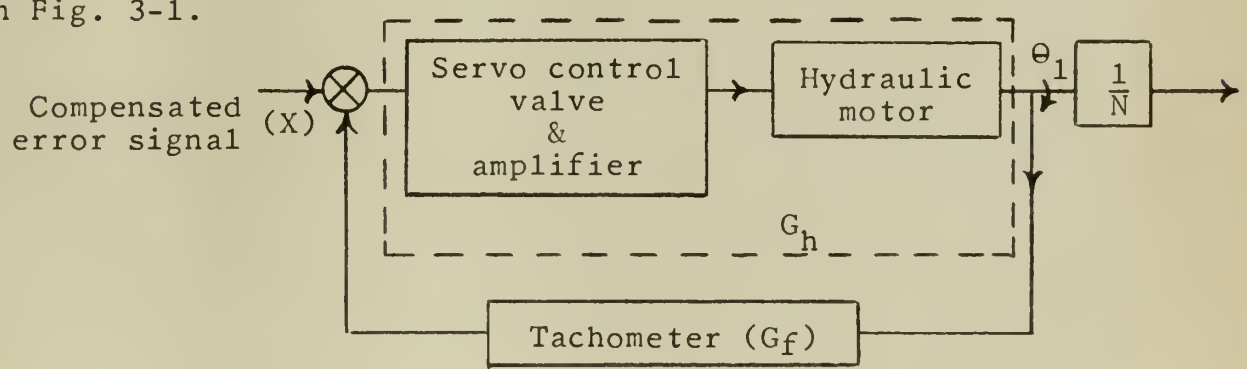

Figure 3-1. Hydraulic drive system.

The transfer function (G_h) is defined as the joint function of the servo amplifier, servo control valve, and hydraulic drive motor. Neglecting the tachometer feedback (G_f), the output position angle to the reduction gearing is (θ_1), where

$$\theta_1 = G_h X \qquad (3\text{-}1)$$

and X is the compensated error signal of the basic system.

The block diagram of the hydraulic drive system with normal antenna loading and external load torque (T_e) due to wind is shown in Fig. 3-2.

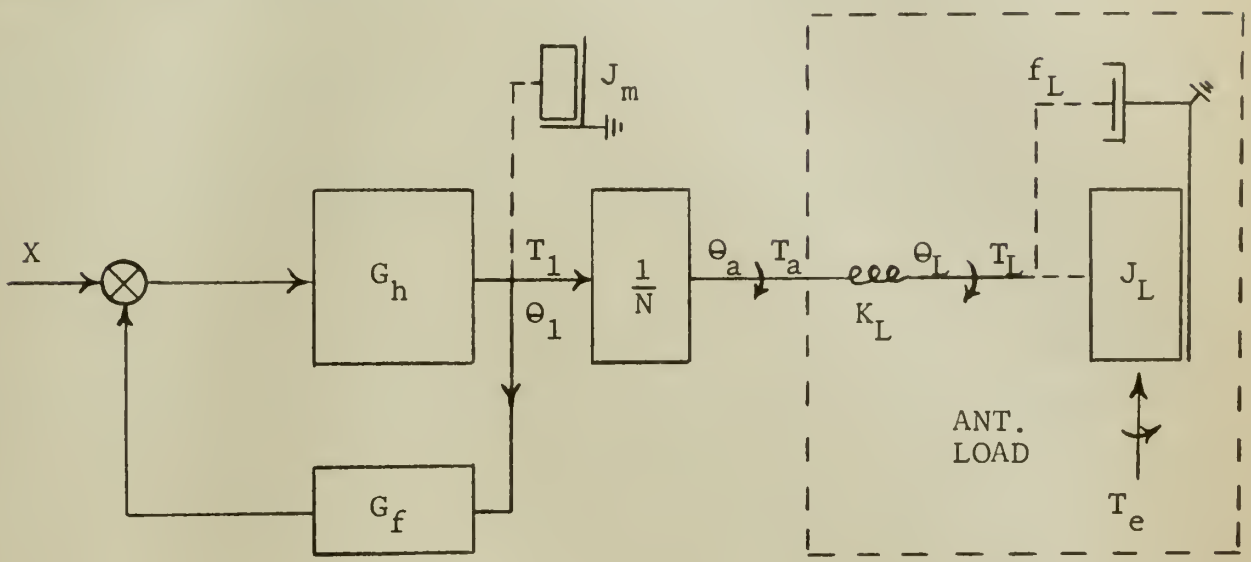

Figure 3-2. Hydraulic system with synthesized loading.

Letting $G_f = 0$,

$$T_1 = T_m + \frac{T_a}{N} = T_m + \frac{T_L}{N} , \qquad (3\text{-}2)$$

where T_m is the torque due to hydraulic motor inertia (J_m) and is defined as

$$T_m = J_m s^2 \Theta_1 . \qquad (3\text{-}3)$$

The load torque (T_L), as shown in Fig. 3-2, is

$$T_L = J_L s^2 \Theta_L + f_L s \Theta_L + T_e = K_L(\Theta_a - \Theta_L) . \qquad (3\text{-}4)$$

$$\Theta_1 = \frac{\Theta_a}{N} , \qquad (3\text{-}5)$$

where N is the gear reduction ratio of the hydraulic system. Substituting equation (3-5) into (3-4) gives

$$T_L = K_L\left(\frac{\Theta_1}{N} - \Theta_L\right) = (J_L s^2 + f_L s)\Theta_L + T_e , \qquad (3\text{-}6)$$

or

$$\theta_L = \frac{K_L}{N(J_L s^2 + f_L s + K_L)} \theta_1 - \frac{1}{(J_L s^2 + f_L s + K_L)} T_e \quad . \tag{3-7}$$

Substituting equation (3-7) into (3-6) gives

$$T_L = \frac{K_L \theta_1}{N} - \frac{K_L^2}{N(J_L s^2 + f_L s + K_L)} \theta_1 + \frac{K_L}{(J_L s^2 + f_L s + K_L)} \quad . \tag{3-8}$$

The flow of oil out of the control valve (Q_v) is considered to be divided into three parts, that lost to system leakage (Q_L), that lost because of compressibility of the oil (Q_c), and that actually used to drive the hydraulic motor (Q_m).

$$Q_v = Q_L + Q_c + Q_m \tag{3-9}$$

The flow out of the control valve is a function of the input error voltage (X) within some constant (K_v) and is defined as

$$Q_v = K_v X \quad . \tag{3-10}$$

The constant (K_v) is defined to include the control valve constant as well as the servo amplifier gain constant. Brown and Campbell in "Principals of Servomechanisms" [2] define the separate oil flows of the system as follows:

$$Q_L = L P \quad , \tag{3-11}$$

where L is the leakage coefficient and P is the pressure differential of the system.

$$Q_c = \frac{V}{B} sP \quad , \tag{3-12}$$

where V is the volume of oil under compression and B is the bulk modulus of the oil.

$$Q_m = dm\ s\Theta_1 \ , \qquad (3\text{-}13)$$

where dm is the motor displacement and Θ_1 is shown in Fig. 3-2. Dimensions of all constants are listed in the table of constants on page 12.

Making substitutions of these flows into equation (3-9) gives

$$K_v X = dm\ s\Theta_1 + (L + \frac{V}{B}s)\ P. \qquad (3\text{-}14)$$

The pressure differential (P) of the system is related to the torque output of the motor (T_1) as follows:

$$T_1 = dm\ P \ . \qquad (3\text{-}15)$$

Substitution of equations (3-15), (3-3), (3-4), into equation (3-2) gives

$$T_1 = dm\ P = J_m s^2\Theta_1 + \frac{K_L}{N^2}\left[\frac{-K_L}{(J_L s^2 + f_L s + K_L)} + 1\right]\Theta_1 + \frac{K_L}{N(J_L s^2 + f_L s + K_L)}\ T_e \ , \qquad (3\text{-}16)$$

or

$$P = \frac{J_m\ s^2}{dm}\ \Theta_1 + \frac{K_L}{dm\ N^2}\ \frac{(J_L s^2 + f_L s)}{(J_L s^2 + f_L s + K_L)}\ \Theta_1 + \frac{K_L}{dm\ N\ (J_L s^2 + f_L s + K_L)}\ T_e \ . \qquad (3\text{-}17)$$

Substitution of equation (3-14) gives

$$K_v X = dm\, s\Theta_1 + \left(L + \frac{V}{B}s\right)\left[\frac{J_m s^2}{dm}\Theta_1 + \frac{K_L\,(J_L s^2 + f_L s)\,\Theta_1}{dm\,N^2(J_L s^2 + f_L s + K_L)}\right] + \frac{\left(L + \frac{V}{B}s\right)K_L}{dm\,N\,(J_L s^2 + f_L s + K_L)} T_e \,. \qquad (3\text{-}18)$$

If the external torque (T_e) is assumed equal to zero, then, solving for $\frac{X}{\Theta_1}$ in equation (3-18) gives

$$\frac{X}{\Theta_1} = \frac{1}{K_v}\left[dm\, s + \left(L + \frac{V}{B}s\right)\frac{J_m s^2}{dm} + \left(L + \frac{V}{B}s\right)\frac{K_L}{dm\,N^2}\,\frac{(J_L s^2 + f_L s)}{(J_L s^2 + f_L s + K_L)}\right].$$

Since $G_h = \frac{\Theta_1}{X}$,

$$G_h = \frac{K_v}{s\left[dm + \left(L + \frac{V}{B}s\right)\frac{J_m}{dm}s + \left(L + \frac{V}{B}s\right)\frac{K_L}{dm\,N^2}\,\frac{(J_L s + f_L)}{(J_L s^2 + f_L s + K_L)}\right]} \,. \qquad (3\text{-}19)$$

Since the system stiffness factor (K_L) is relatively large, equation (3-19) reduces to

$$G_h = \frac{BK_v\, dm \,/\, V(J_m + J_L/N^2)}{s\left[s^2 + \left(\frac{LB}{V} + \frac{f_L}{N^2(J_m + \frac{J_L}{N^2})}\right)s + \frac{LBf_L}{N^2(J_m + \frac{J_L}{N^2})} + \frac{dm^2\, B}{V(J_m + \frac{J_L}{N^2})}\right]} \,. \qquad (3\text{-}20)$$

The friction coefficient of the antenna drive is considered very small with respect to the load inertia constant, thus,

$$\frac{f_L}{N^2(J_m + \frac{J_L}{N^2})} \cong 0 \,,$$

and equation (3-20) reduces to

$$G_h = \frac{N^2 K_v B\ dm\ /\ V(J_L + N^2 J_m)}{s\left[s^2 + \frac{LBs}{V} + \frac{N^2\ dm^2\ B}{V(J_L + N^2 J_m)}\right]} \quad . \qquad (3\text{-}21)$$

The hydraulic constants associated with this system are as follows:

$N = 2160$

$K_v = 0.895$

$J_L = 4.2 \times 10^6$ lb-in-sec^2 (referred to antenna)

$J_m = 0.09$ lb-in-sec^2 (referred to motor)

$B = 0.27 \times 10^6$ psi

$L = 60.5 \times 10^{-5}$ in^3/sec/psi

$V = 3.9$ in^3

$dm = 0.215$ in^3/radian

Substituting these constants into equation (3-21) gives

$$G_h = \frac{1.345 \times 10^4}{s(s^2 + 42s + 3228)} \quad . \qquad (3\text{-}22)$$

Equation (3-22) is the transfer function of the uncompensated hydraulic system and was used in the initial development of the complete basic system which follows. The transfer functions of the complete basic system chosen initially for investigation are shown in Fig. 3-3. The values shown for the individual transfer functions were suggested by the manufacturer as representing the azimuth control system for the antenna under investigation. The open-loop transfer function (F_o) and the closed-loop function (F_c) for the system of

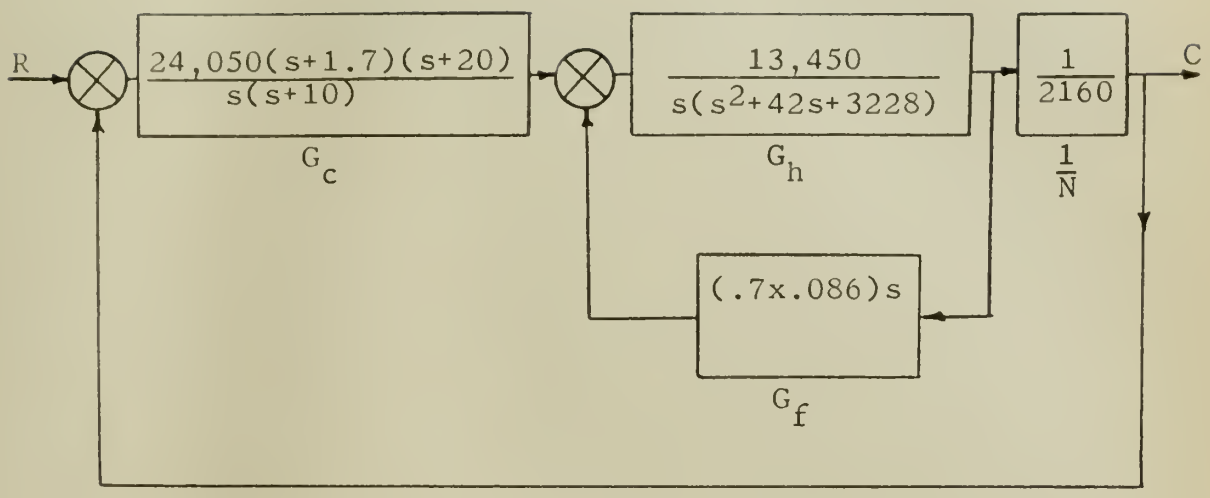

G_c = Cascade compensation

G_h = Hydraulic drive

G_f = Tachometer feedback (tachometer constant = .086)

N = Gear ratio (2160)

Figure 3-3

Block diagram of initial basic system.

Fig. 3-3 are as follows:

$$F_o = \frac{14.96 \times 10^4 (s + 1.7)(s + 20)}{s^2(s + 10)(s^2 + 42s + 4038)} \qquad (3\text{-}23)$$

$$F_c = \frac{14.96 + 10^4 (s + 1.7)(s + 20)}{s^5 + 52s^4 + 4458s^3 + 1.8988\times10^5 s^2 + 3.24\times10^6 s + 5.08\times10^6} \cdot \qquad (3\text{-}24)$$

4. Analysis of basic system.

In order to ascertain the stability of the system of Fig. 3-3, a Routh's criterion test was made of the closed-loop transfer function (F_c).

Routh's criterion test:

1	4.458×10^3	3.24×10^6
52	1.8988×10^5	5.08×10^6
810	3.14×10^6	0
-1.172×10^4	5.08×10^6	0
3.49×10^6	0	0
5.08×10^6	0	0

The system as given was believed stable, but Routh's criterion test did not verify this assumption. Accordingly, a Nyquist plot was drawn of the system transfer function in order to observe the degree of instability and is shown in Fig. 4-1. Within the accuracy of the plot, the curve appeared to pass through the Nyquist point indicating marginal stability. For further investigation of the system stability, a Bode plot, using asymptotes only, of F_o was constructed and is shown in Fig. 4-2. Although the plot crossed the zero db line with a negative six db slope, the complex poles of F_o, having a natural frequency (w_n) of 63.5 rad/sec, caused a hump in the plot which, if the magnitude were sufficiently large, would recross the zero db line and result in system instability.

In order to estimate the maximum amplitude of the hump, that part of the system transfer function ($\hat{F}$) resulting from

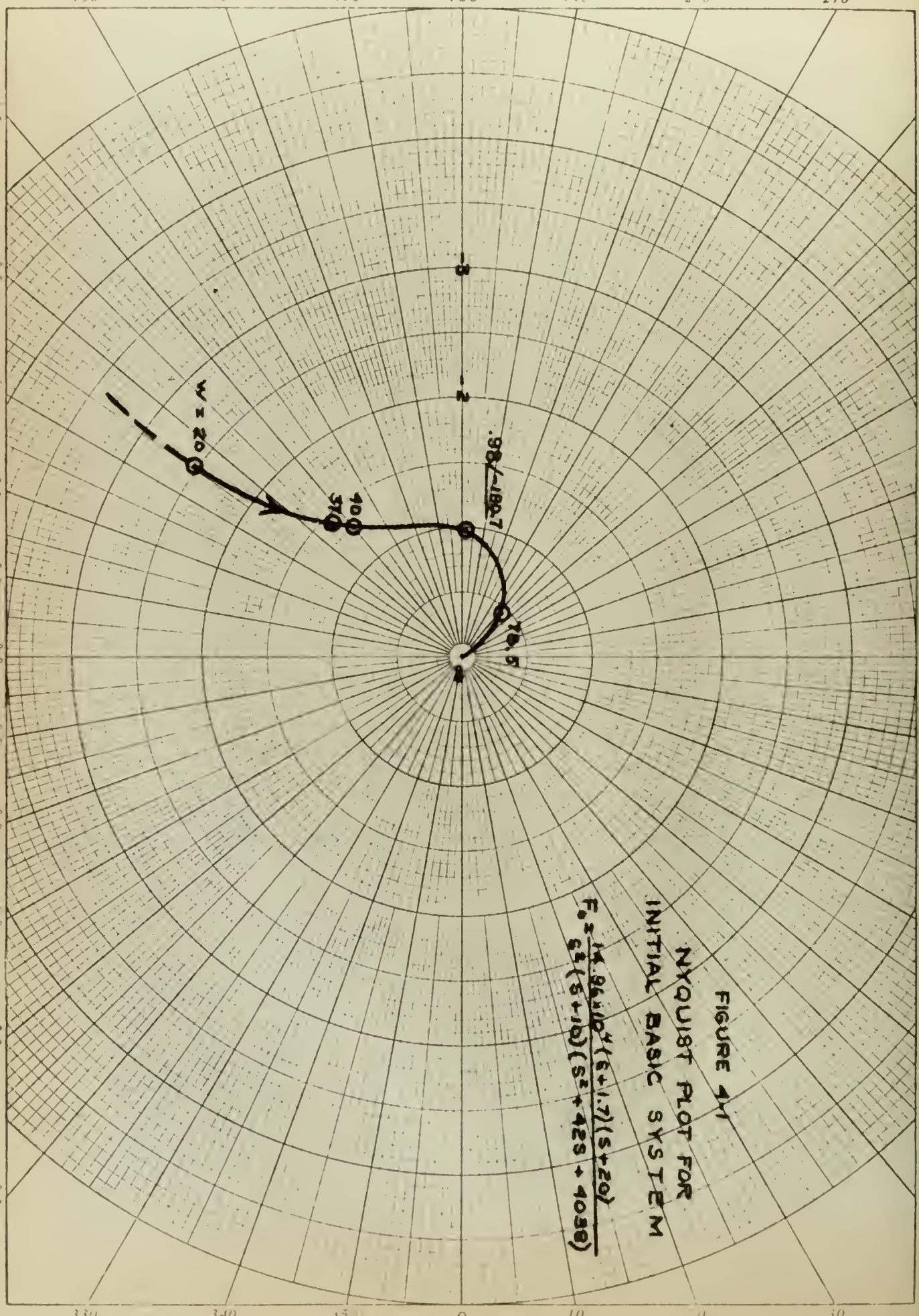

FIGURE 4.1
NYQUIST PLOT FOR
INITIAL BASIC SYSTEM

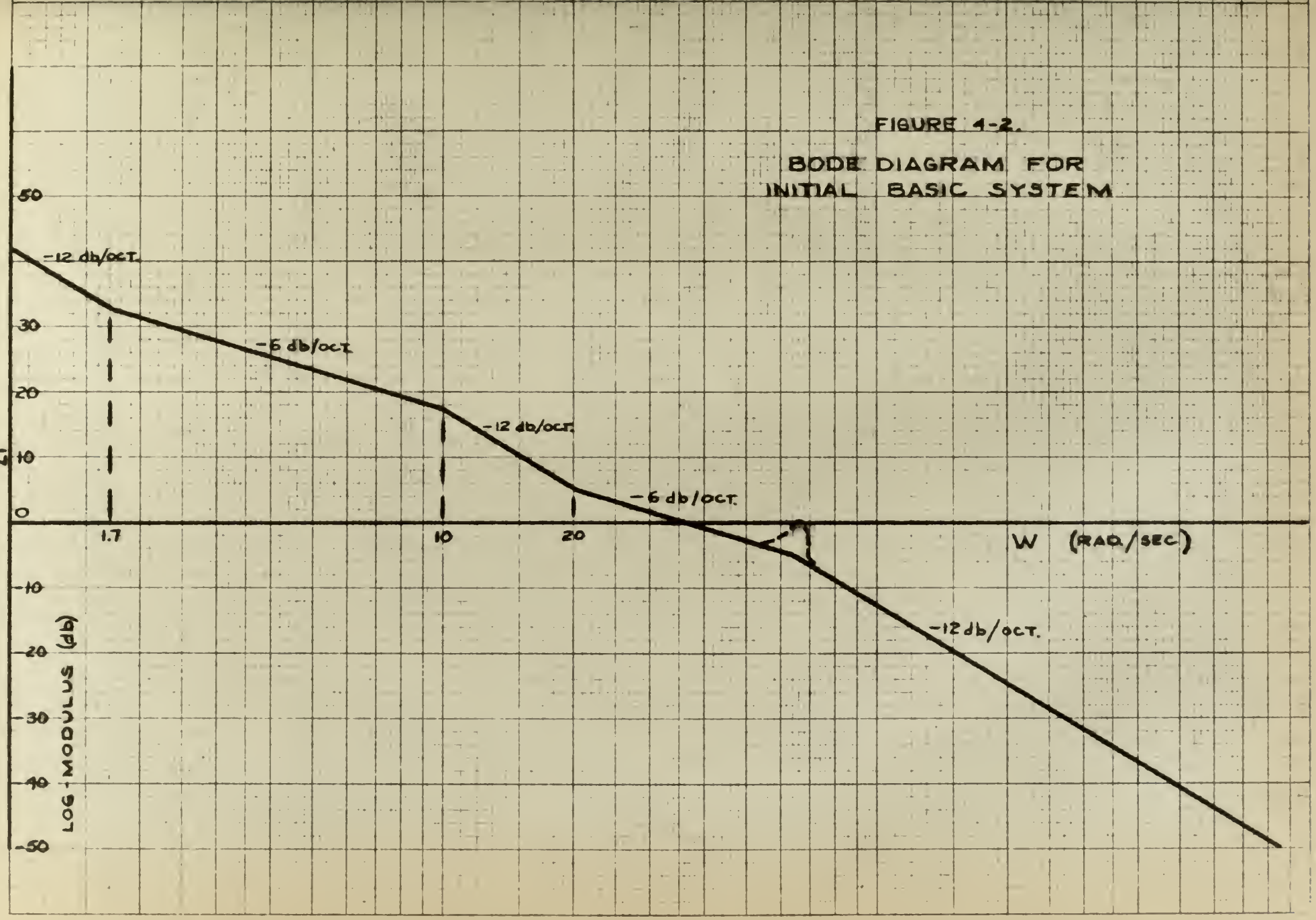

FIGURE 4-2.

BODE DIAGRAM FOR
INITIAL BASIC SYSTEM

the complex poles can be written in vector form as [1]

$$\hat{F} = \frac{1}{(1 - \frac{w}{w_o}^2) + j2\zeta\frac{w}{w_o}} = Me^{jN} , \qquad (4\text{-}1)$$

where: w_o = break frequency of the complex poles

ζ = damping coefficient

$M = |\hat{F}|$

N = phase angle of $\hat{F}$

The maximum absolute value of $\hat{F}$ (M_{max}) is the maximum amplitude of the hump. Letting $\frac{w}{w_o} = u$ and substituting into equation (4-1) gives

$$\hat{F} = \frac{1}{(1 - u^2) + j2\zeta u} ,$$

or

$$M = \frac{1}{\sqrt{(1 - u^2) + 4\zeta^2 u^2}} . \qquad (4\text{-}2)$$

Differentiating equation (4-2) with respect to u gives

$$\frac{dM}{du} = \frac{-2(1 - u^2)(-2u) + 8\zeta^2 u}{2\left[(1 - u^2)^2 + 4\zeta^2 u^2\right]^{\frac{1}{2}}\left[(1 - u^2)^2 + 4\zeta^2 u^2\right]} . \qquad (4\text{-}3)$$

Setting equation (4-3) equal to zero and solving for u gives

$$u = (1 - 2\zeta^2)^{\frac{1}{2}} . \qquad (4\text{-}4)$$

Substituting equation (4-4) into (4-2) yields

[1] Chestnut and Mayer, Servomechanisms and Regulating Systems Design, Vol I, pp 312, September 1953.

$$M_{max} \cong \frac{1}{2\zeta(1-\zeta^2)^{\frac{1}{2}}} \quad . \qquad (4\text{-}5)$$

Equation (4-5) is an approximation of M_{max} since it was developed on the basis that the frequency at M_{max} was equal to the break frequency (w_o). However, these two frequencies differ slightly.

The damping factor (ζ) can be computed from equation (3-23) as

$$2\zeta w_n = 42 \ ,$$

where $w_n = (4038)^{\frac{1}{2}}$, or $\zeta = 0.33$.

Therefore, from equation (4-5)

$$M_{max} = 1.7 = 4.62 \text{ db} \ .$$

The maximum amplitude of the hump, 4.62 db, was added to the amplitude at the complex pole break frequency in Fig. 4-2 and resulted in a system amplitude at this frequency of 0.12 db.

Although the above calculation is not exact, it at least shows the hump quite close to the zero db line and thus, the system has a very small stability margin at best. A decrease in system gain would improve the stability by lowering the hump below the zero db line, but as only 5.5 db can be dropped before the slope crossing the zero db line decreases to -12 db, this approach is not satisfactory.

The above marginal stability was a result of the location of the complex poles of F_o. These poles in turn were placed by the location of the complex poles of the hydraulic drive transfer function (G_h) and the tachometer feedback (G_f). Near

cancellation of these latter poles was achieved by insertion of a complex-zero compensator (G_o) in series with G_h, alleviating the instability problem. The design of the complex-zero compensator appears in Appendix I.

Equation (3-22) has shown the complex poles of G_h to be $(s^2 + 42s + 3228)$. The form of the transfer function of the complex-zero compensator (G_o) is shown by equation (I-9) in Appendix I. Thus, the G_o necessary to cancel the complex poles of G_h is

$$G_o = \frac{1}{3228} (s^2 + 42s + 3228).$$

For the purpose of this study, complete cancellation of the complex poles of G_h was assumed. In the actual application, some residue would remain since equation (I-9) does not exactly represent the transfer function of the compensator in Fig. I-1 of the Appendix.

Placing G_o in series with G_h inside the tachometer feedback loop results in a new open-loop transfer function,

$$F_o = \frac{37 (s + 1.7)(s + 20)}{s^2 (s + 10)} . \qquad (4\text{-}6)$$

Fig. 4-3 shows the Bode diagram of the function of equation (4-6). A comparison of this Bode with Fig. 4-2 shows that the desired cancellation has been achieved without change of the system gain or location of the remaining break points. Thus, the system response remains the same with the exception of the undesirable effect of the complex poles.

At this point, a limitation was placed on the system

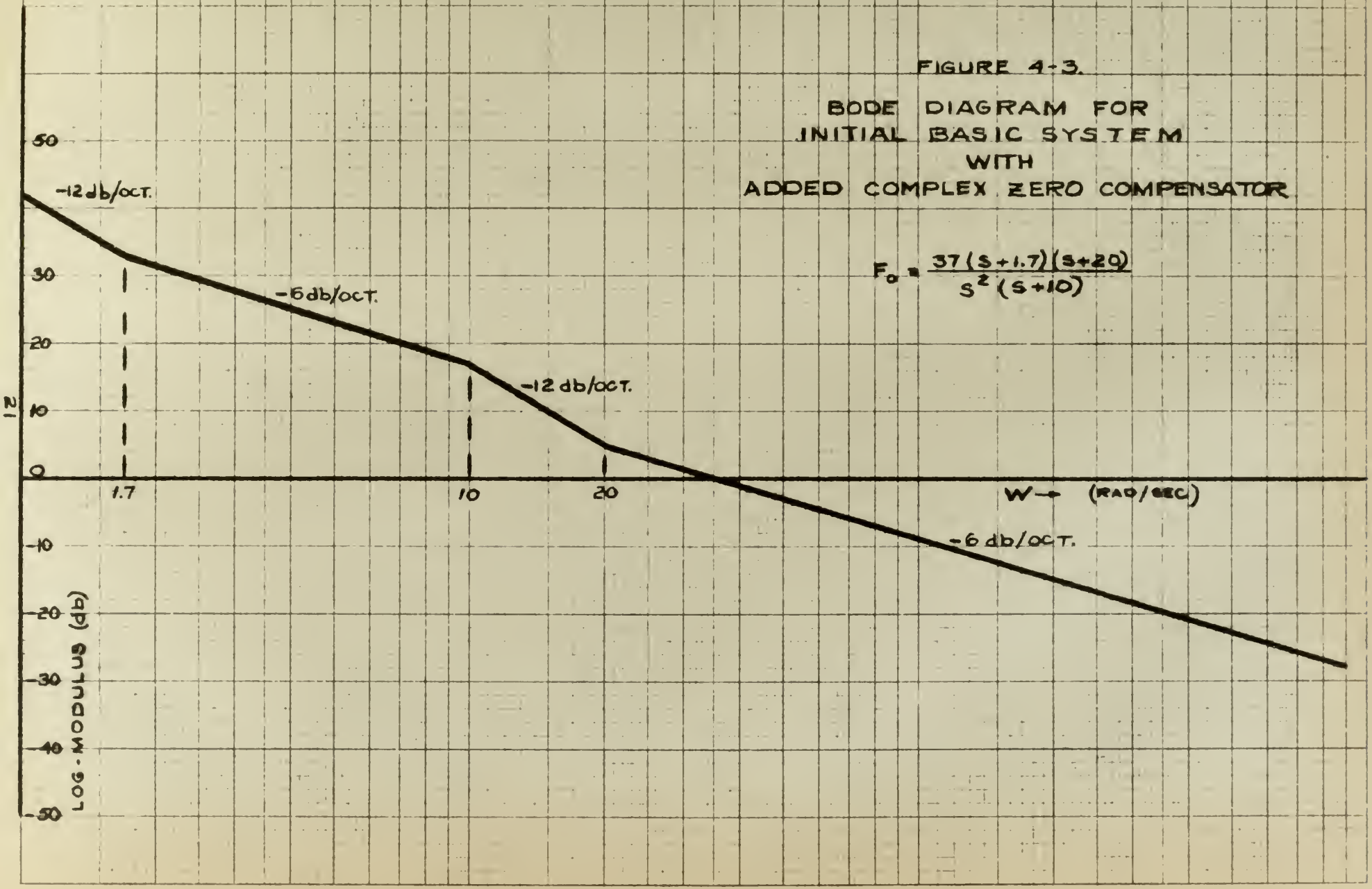

FIGURE 4-3.

BODE DIAGRAM FOR
INITIAL BASIC SYSTEM
WITH
ADDED COMPLEX ZERO COMPENSATOR

$$F_o = \frac{37(S+1.7)(S+20)}{S^2(S+10)}$$

cascade compensation (G_c). In order that components of less stringent design might be utilized in G_c, the cascade gain of 2.405×10^4 was limited to a value of 1×10^3. In order that the system gain of equation (4-6) be retained, servo amplifier gain of the hydraulic system as well as tachometer feedback gain were modified through the following development.

The open-loop transfer function of the basic system of Fig. 4-4 is

$$F_o = \frac{G_c}{N} \left(\frac{G_o G_h}{1 + G_o G_h G_f} \right) . \qquad (4\text{-}7)$$

Equating the system gains of equation (4-7) with the desired system gain of equation (4-6) gives

$$\frac{K_c}{N} \left(\frac{K_o K_h}{1 + K_o K_h K_f} \right) = 37 , \qquad (4\text{-}8)$$

where K represents the gain constants of the subscripted transfer functions of equation (4-7). Substituting $K_c = 1000$ in equation (4-8) gives

$$\frac{K_o K_h}{1 + K_o K_h K_f} = \frac{37 \times 2160}{1000} = 80 . \qquad (4\text{-}9)$$

Substituting $K_f = 0.7 \times 0.086$, where 0.086 is the tachometer constant, into equation (4-9) gives

$$(1 - .7 \times .086) K_o K_h = 80$$

or

$$K_o K_h = -20.95 . \qquad (4\text{-}10)$$

Since all transfer function gains must be positive, equation (4-10) indicates that the tachometer gain must be changed in order to realize the desired overall system gain. In order that $K_o K_h$ be a positive number, equation (4-10) demands

$$(1 - 80K_f) \geq 0 \ . \qquad (4\text{-}11)$$

Since the tachometer constant (.086) can not be changed, the tachometer gain must be changed so that its value is less that 0.1455 in order that $K_o K_h$ be positive. To ensure this positive value, a tachometer gain of 0.135 was selected.

$$K_f = .135x.086 \ ,$$

and

$$(1 - .135x.086x80)K_o K_h = 80 \ , \qquad (4\text{-}12)$$

or

$$K_o K_h = 1150$$

where $K_o = \frac{1}{3228}$; therefore

$$K_h = 1150x3228 = 3.72x10^6 \ . \qquad (4\text{-}13)$$

Equation (3-21) defined K_h as

$$K_h = \frac{N^2 \ B \ dm \ K_v}{V(J_L + N^2 J_m)} = 1.528x10^4 \ K_v \ . \qquad (4\text{-}14)$$

Substitution of equation (4-13) into (4-14) gives

$$K_v = 245$$

where K_v was previously defined as including the control

valve constant as well as the variable servo amplifier gain.

The transfer functions of the basic system reflecting the above changes are

$$G_h = \frac{3.72 \times 10^6}{s(s^2 + 42s + 3228)}$$

$$G_o = \frac{1}{3228}(s^2 + 42s + 3228)$$

$$G_f = (.135 \times .086)s$$

$$G_c = \frac{1000\ (s + 1.7)(s + 20)}{s(s + 10)} \ .$$

The new open-loop transfer function (F_o) was shown in equation (4-6). The new closed-loop transfer function was derived:

$$F_c = \frac{37\ (s + 1.7)(s + 20)}{(s + 1.74)(s^2 + 45.26s + 724.4)} \ . \qquad (4\text{-}15)$$

This is the basic system transfer function referred to hereafter as G_1 and is shown in Fig. 4-4.

As was shown in the development of the basic approach, the conditional feedback compensation effects only the disturbance response of the basic system. Fig. 4-5 shows the response of the basic system to a unit step disturbance input (U), where,

$$C = \frac{1}{1 + F_o} U \ .$$

The response curve of Fig. 4-5 was plotted using the transient

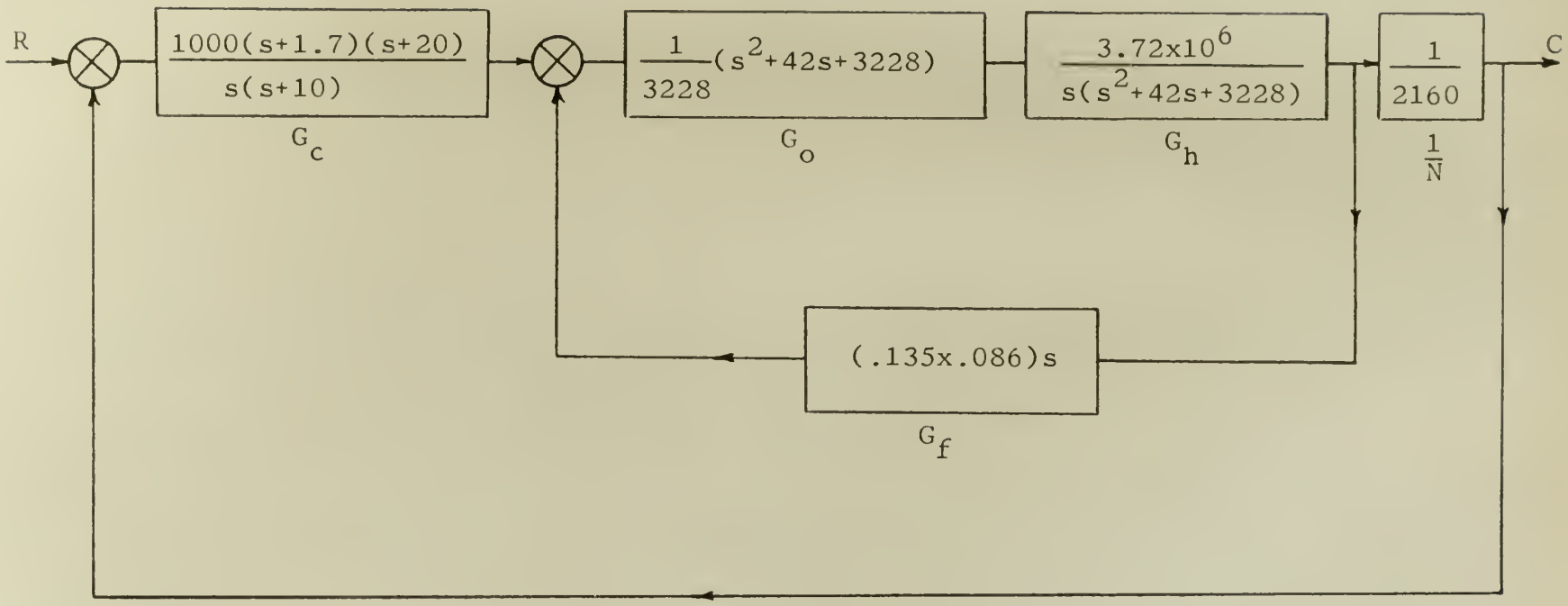

Figure 4-4. Block diagram of basic system with complex zero compensator and gain modifications.

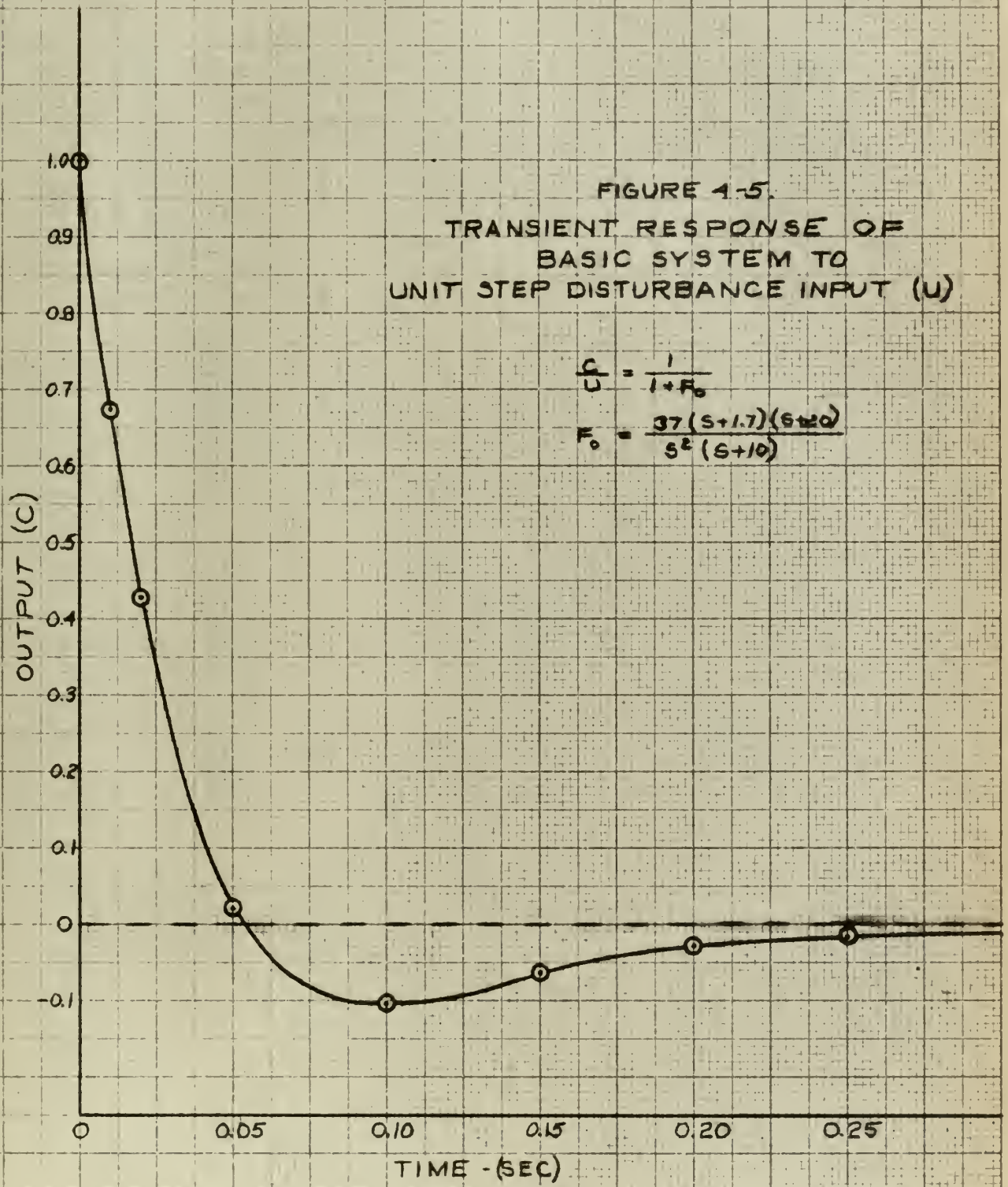

FIGURE 4-5.
TRANSIENT RESPONSE OF
BASIC SYSTEM TO
UNIT STEP DISTURBANCE INPUT (U)

$$\frac{C}{U} = \frac{1}{1+F_o}$$

$$F_o = \frac{37(S+1.7)(S+20)}{S^2(S+10)}$$

FIGURE 4-6.

DISTURBANCE - OUTPUT FREQUENCY RESPONSE OF BASIC SYSTEM

$$\frac{C}{U} = \frac{1}{1 + F_o}$$

$$F_o = \frac{37(S+1.7)(S+20)}{S^2(S+10)}$$

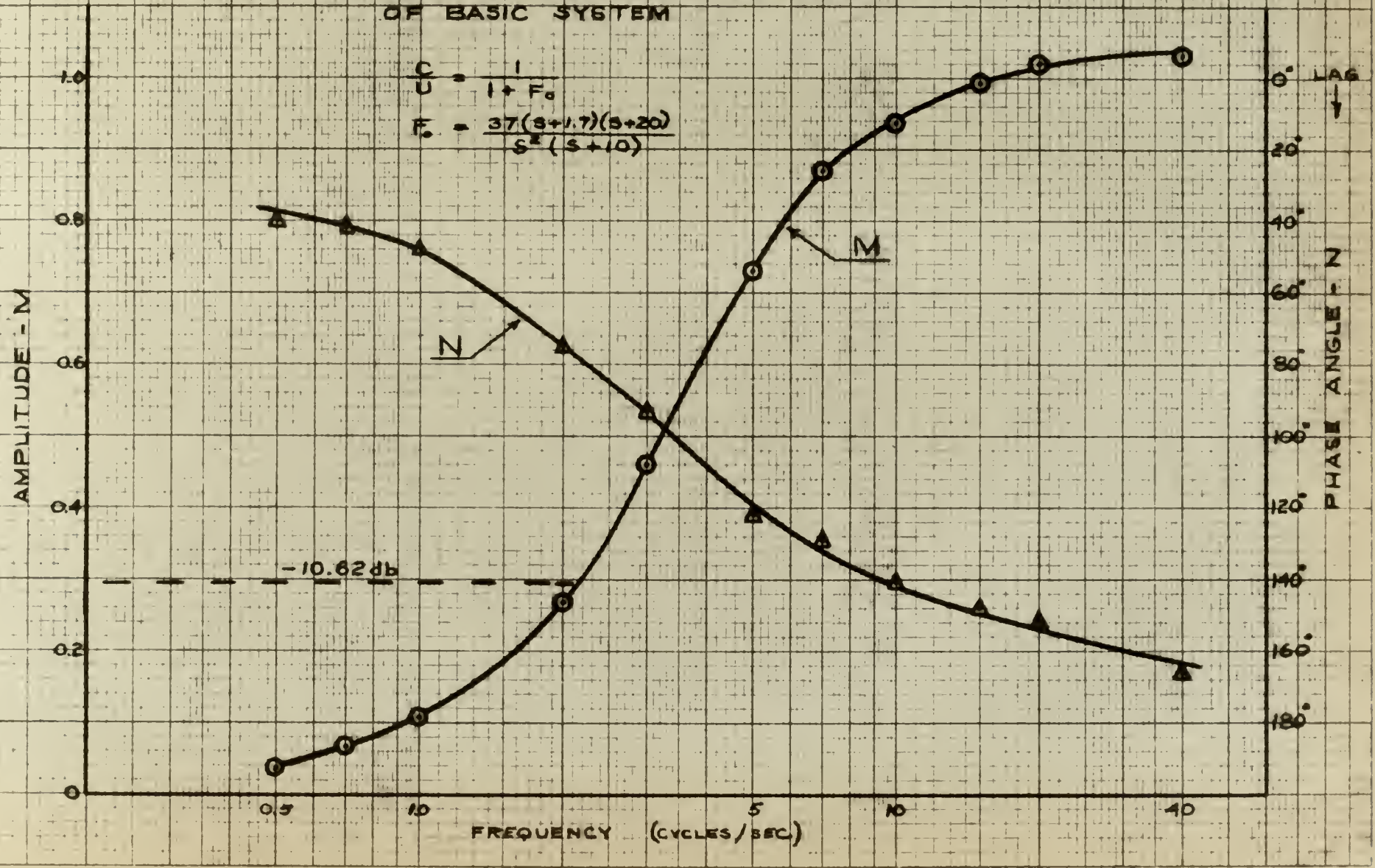

response equation determined by the graphical residue technique. The details of this procedure are included in Appendix II. The maximum overshoot in Fig. 4-5 is 10.3% and occurs at t = 0.10 seconds. Fall-time, defined as the time interval between ten percent and 90 percent decay during the initial cycle of response, is 0.037 seconds. The conditional feedback compensation to be attempted will try to reduce significantly this fall time.

Fig. 4-6 shows the frequency response of the basic system to a disturbance input of from 0.5 cps. to 40 cps. It is noted that as the frequency of the disturbance input signal is increased, the regulating effect of the basic system deteriorates. In order to compare this frequency response with that resulting after conditional feedback compensation, the system bandwidth is defined as that frequency above which the input disturbance is attinuated by less than 10.62 db, or where M is equal to (1 - .707). In Fig. 4-6 this value of amplitude is reached at a frequency of 2.10 cycles per second. The corresponding phase angle is (-)78 degrees.

5. Development of compensation technique.

The following is a derivation of the conditional compensated disturbance-output transfer function together with a presentation of a compensation technique. Fig. 5-1 is a block diagram showing the inputs and transfer blocks of the proposed conditional feedback compensated system, where

$G_1 = \frac{F_o}{1 + F_o}$, the closed loop transfer function of the basic system

F_o = the open loop transfer function of the basic system

G_2 = compensator to be determined

R = tracking input information

U = load disturbance information

C = system output

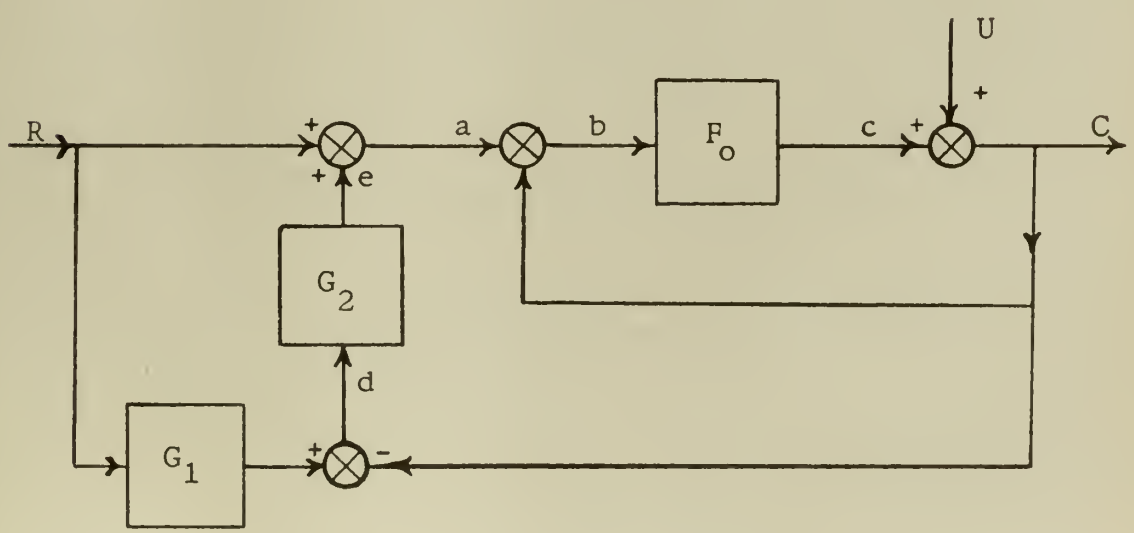

Figure 5-1. Block diagram of proposed conditional feedback system.

The transfer function of the output (C) with respect to R and U is developed from Fig. 5-1. The relations below follow from Fig. 5-1.

$$C = U + c = U + (a - C)F_o$$

$$c = bF_o = (a - C)F_o$$

$$b = a - C$$

$$d = RG_1 - C$$

$$e = RG_2G_1 - CG_2$$

$$a = R + e = R + RG_2G_1 - CG_2$$

Combining these relationships gives

$$C = U + (R + RG_2G_1 - CG_2 - C)F_o \ . \qquad (5\text{-}1)$$

Rearrangement of equation (5-1) gives

$$C = \frac{U}{1 + F_o + F_oG_2} + \frac{(1 + G_1G_2)F_o}{1 + F_o + F_oG_2} R \ . \qquad (5\text{-}2)$$

Since $1 + F_o = \frac{F_o}{G_1}$, then equation (5-2) becomes

$$C = \frac{U}{\frac{F_o}{G_1} + F_oG_2} + \frac{(1 + G_1G_2)F_o}{\frac{F_o}{G_1} + F_oG_2} R$$

$$C = \frac{1}{\frac{F_o}{G_1}(1 + G_1G_2)} U + \frac{(1 + G_1G_2)F_o}{\frac{F_o}{G_1}(1 + G_1G_2)} R$$

$$C = \frac{1}{(1 + F_o)(1 + G_1G_2)} U + G_1R \qquad (5\text{-}3)$$

Therefore, the output due to load disturbance (U) is:

$$\left[\frac{1}{1 + F_o}\right]\left[\frac{1}{1 + G_1G_2}\right] U. \qquad (5\text{-}4)$$

The output due to the tracking input (R) is:

$$G_1R \ . \qquad (5\text{-}5)$$

The input-output transfer function G_1 is the same as that for the uncompensated basic system. Thus, this input-output response remains unchanged with the addition of the compensation.

Root-locus techniques are to be used to select a G_2 which will give a desired disturbance-output response. The disturbance-output transfer function may be written in the following form to facilitate the application of the root-locus technique.

$$\left[\frac{1}{1 + F_o}\right]\left[\frac{1}{1 + G_1G_2}\right] = \frac{1}{1 + F_o + F_oG_2} = \frac{D_oD_2}{D_oD_2 + N_oN_2 + N_oD_2} \qquad (5\text{-}6)$$

where:

$$F_o = \frac{N_o}{D_o}$$

$$G_1 = \frac{F_o}{1 + F_o} = \frac{N_o}{(N_o + D_o)}$$

$$G_2 = \frac{N_2}{D_2}$$

The denominator of the above function requires two root loci in order to determine the final closed-loop roots of the disturbance-output transfer function. Since it is desired to investigate the effects of several values of the compensator G_2, it seemed advantageous if a function, closely representing the disturbance-output function, could be utilized which would require only one root-locus plot to place the roots of the closed-loop function. An examination of the function

$\frac{1}{1 + G_1G_2}$ shows it to be such a function. This function can be rewritten as

$$\frac{1}{1 + G_1G_2} = \frac{1 + F_o}{1 + F_o + F_oG_2} = \frac{D_1D_2}{D_1D_2 + N_1N_2} , \qquad (5\text{-}7)$$

where $G_1 = \frac{N_1}{D_1}$.

The roots of the function of equation (5-7), hereafter referred to as the "representing function," are the same as that for the desired disturbance-output function of equation (5-6). Furthermore, this function is of a form which requires the use of only one root locus in order to place the roots of the desired closed-loop function. Thus, if a direct correlation between the representing function and the desired function can be shown, the problem of selecting G_2 through simple root-locus techniques is made relatively easy. The development of this correlation follows.

The representing function of equation (5-7) can also be written as

$$\frac{1}{1 + G_1G_2} = \frac{D_oD_2 + N_oD_2}{D_oD_2 + N_oD_2 + N_oN_2} .$$

For the basic type 2 system given, D_o takes the form:

$$s^2(\tau_1 s + 1)(\tau_2 s + 1) \ldots \ldots$$

and represents the denominator of the open-loop transfer function of the basic system.

Assuming the compensator (G_2) takes the form:

$$\frac{s^m(\tau_1 s + 1)(\tau_2 s + 1)}{(\tau_3 s + 1)(\tau_4 s + 1)} \ldots \ldots \quad , \; m \geq 0,$$

then the numerator of the representing function, ($D_oD_2 + N_oD_2$), is some polynomial in s of the form

$$(As^n + Bs^{n-1} + \ldots \ldots + D) .$$

The denominator of the representing function is also of the same general form, ($A's^p + B's^{p-1} + \ldots \ldots + D'$). Since no factored s term exists in either the numerator or denominator, the response to a step input of this representing function will include a residue at the "input" pole inserted at the origin and, therefore, will have a steady-state error constant. The desired disturbance-output function has been shown in equation (5-6) to be:

$$\frac{D_oD_2}{D_oD_2 + N_oD_2 + N_oN_2} \quad , \text{ which is of the form:}$$

$$\frac{s^2(\tau_1 s + 1)(\tau_2 s + 1) \ldots (\tau_3 s + 1)(\tau_4 s + 1)}{A's^p + B'^{p-1} + \ldots + D'} .$$

Since this form does not produce a residue at the origin of the s plane due to a step input, the time response has no error constant.

The time response of the representing function to a step input is of the form:

$C_1 + C_2 e^{-\alpha_1 t} \sin(w_c t + \psi)$, to a second order approximation. As time increases, the value of the output of the representing function will tend to be larger by an amount C_1 than that expected for the desired function in which C_1 is equal to zero.

If there exists no phase difference (γ) between the representing function and the desired function, then to a second order approximation, the correlation would simply be:

$$\frac{1}{1 + G_1G_2} A\, u(t) - C_1 \cong \left[\frac{1}{1 + F_o}\right]\left[\frac{1}{1 + G_1G_2}\right] A\, u(t).$$

This, of course, is not the case. Some phase difference between the two functions must exist since they are not identical. It is this phase difference (γ) between the functions which in addition to the constant error term, decides the similarity between the two functions. Some correlation with respect to this phase difference is necessary.

An inspection of the desired transfer function,

$$\left(\frac{1}{1 + F_o}\right)\left(\frac{1}{1 + G_1G_2}\right) = \frac{D_oD_2}{D_oD_2 + N_oD_2 + N_oN_2} ,$$

shows that the zeros of this function are made up of the poles of F_o and G_2. An inspection of the representing function,

$$\left(\frac{1}{1 + G_1G_2}\right) = \frac{D_2(N_o + D_o)}{D_oD_2 + N_oD_2 + N_oN_2} ,$$

shows this function to have zeros that are made up of the poles of G_1 and G_2. Both functions contain zeros which are the poles of G_2. In addition, both functions have the same roots. The only difference between the time response of these functions must be due to the difference between the placement of the poles of F_o and the poles of G_1, $(N_o + D_o)$, the remaining zeros of the two functions. To a second order approximation, the phase difference (γ) can be determined by noting the placement of the poles of F_o and G_1 with respect to the complex pole of either the representing or desired function, since they are identical. The phase difference (γ), determined using graphical residue methods, is as follows:

γ = Sum of the angles from the poles of F_o to the complex pole of the representing function minus the sum of the angles from the poles of G_1 to the complex pole of the representing function. (5-8)

Since the response of the representing function to a unit step input, to a second order approximation, is of the form

$$C_1 + C_2e^{-\alpha_1 t} \sin(w_c t + \psi) , \qquad (5-9)$$

then the response of the desired function to a unit step

input must be,

$$C_3 e^{-\alpha_1 t} \sin(w_c t + \Psi + \gamma). \qquad (5\text{-}10)$$

The development thus far permits the determination of the correlating parameters, phase difference (γ) and steady-state error constant (C_1). Techniques for utilizing these parameters to predict the desired response from the representing response are presented in the following development.

A comparison of equations (5-9) and (5-10) show that they differ by a constant, a proportionality factor, and a phase difference (γ). The value of C_1 can be determined to a second order approximation and is shown below.

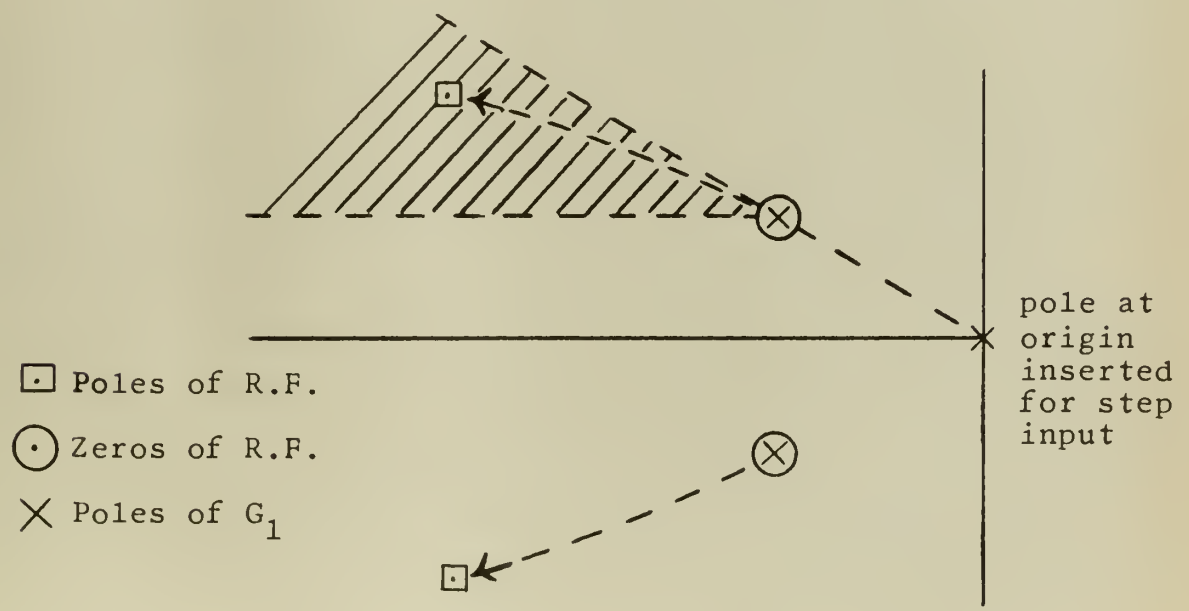

Figure 5-2. Representing function pole and zero placement.

The representing function, referred to hereafter in this section as R.F., has pole and zero locations as shown in Fig. 5-2. Applying graphical residue techniques to Fig. 5-2 for a unit step input gives

C_1 = Distance to zeros of R.F. from the origin divided by the distance to the complex poles of R.F. from the origin.

Since G_2 is chosen such that R.F. approximates a second order system, the zeros of R.F. are equal to the poles of G_1, thus

$$C_1 \cong \left[\frac{W_n(G_1)}{W_n(R.F.)}\right]^2 \qquad (5\text{-}11)$$

where $W_n(G_1)$ is the distance from the complex poles of G_1 to the origin and $W_n(R.F.)$ is the distance from the complex poles of R.F. to the origin. Equation (5-11) shows, for example, that if the compensated response is to be three times as fast as that of G_1, then $W_n(R.F.)$ should be approximately three times that of $W_n(G_1)$. In this example,

$$C_1 \cong (\tfrac{1}{3})^2 \cong .11$$

Thus, for a significant improvement in response time, C_1 will be small. If the phase difference (γ) is also small, C_2 is approximately equal to C_3 since both equations (5-9) and (5-10) must equal unity at zero-plus time. With both C_1 and γ small the response to a unit step input of the desired function will be similar to that of the R.F. For small C_1 and γ the overshoot of the desired function may be predicted. The overshoot of the R.F. to a second order approximation can be determined from the root locus using simple second order techniques. The value of C_1 is then added to this estimate of R.F. overshoot and is used as the prediction of desired function overshoot.

Equation (5-10) shows the phase angle of the desired function to be equal to the sum of Ψ and γ. The value of γ together with its sign was computed using equation (5-8). If a prediction of the desired response based on the R. F. response is to be made, some knowledge of Ψ is necessary in order that the effect of γ, the phase difference, may be known. For example, let Ψ be a second quadrant angle and γ be positive. During the initial period of response, the sine term of equation (5-10) will take on smaller values than will the sine term of equation (5-9). This is to say that for small C_1, the response of the actual desired function will be somewhat faster than that of the R. F. Similar examples can be given for negative γ or for Ψ in different quadrants. Suffice it to say that a knowledge of the quadrant location of Ψ is necessary. The shaded area of Fig. 5-2 defines an area where the location of the complex poles of R. F. produce a Ψ always in the second quadrant. This area is defined in terms of known parameters. It is that area which lies to the left of the complex pole of G_1, where any complex root of R. F. will have a damping factor (σ) greater than or equal to that of G_1, and will have a damped frequency of oscillation (w_c) greater than that of the complex poles of G_1. This area, in general, represents the possible locations of the complex pole of R. F. which will produce a faster response than G_1 but will not effect an increase in overshoot since the damping factor is at least as great as that for G_1. Thus, the most probable location for placement of the

poles of R.F. lies in an area in which Ψ is known to be a second quadrant angle. For complex poles of R.F. in this area, the determination of a positive γ will predict a faster response and a negative γ will predict a slower response of the desired function as compared to the representing function (R.F.). As the absolute value of γ increases, the responses of the two functions become more dissimilar.

Accuracy of the prediction of the desired response from the representing response is gained with experience in using this technique. The steps utilizing the "representing function technique" for determination of the conditional feedback compensation G_2 are summarized below.

1. Specify the desired disturbance response of the compensated system with respect to the original basic system response.
2. Utilize the root-locus method to determine a G_2 that will place the closed-loop poles of R.F. in a position such that desired specifications are approximately met and the R.F. response is approximately of second order.
    a. Place poles in that defined area in which Ψ is a second quadrant angle.
    b. Choose W_n of R.F. complex poles such that $\frac{W_n(R.F.)}{W_n(G_1)}$ is equal to the desired improvement in the response time.
    c. Pick a damping factor to meet desired overshoot requirement.

3. Determine correlation parameters.

   a. Compute $C_1 \cong \left[\frac{W_n(G_1)}{W_n(R.F.)}\right]^2$

   b. Compute γ using rule of equation (5-8).

4. Make first prediction of desired function overshoot.

   a. Using second order approximation technique, estimate overshoot of R.F.

   b. Sum the estimated R.F. overshoot and C_1.

5. Predict the desired function fall-time.

   a. Estimate fall-time of R.F. response as,

   $$\text{fall-time (R.F.)} = \text{fall-time } (G_1) \times \frac{W_n(G_1)}{W_n(R.F.)} \qquad (5\text{-}12)$$

   b. Predicted fall-time of the desired function response is the above estimate modified by γ. Positive γ predicts less fall-time and negative γ predicts greater fall-time than that of the R.F. response. The degree of modification is proportional to the absolute value of γ.

6. Make second prediction of desired function overshoot.

   a. Increase first predicted value if γ is positive and decrease if negative. The degree of modification is proportional to the absolute value of γ.

7. Compare predicted response with specified desired disturbance response. If satisfactory, proceed to verify response of the actual system including the G_2 conditional feedback compensator.

6. Determination of conditional feedback compensator.

The representing function, $\frac{1}{1 + G_1G_2}$, will be used to determine the specific G_2 compensation through root-locus techniques in the manner outlined in Section 5. Observation of the response of the basic system to unit step disturbance, Fig. 6-1, shows it to have the following characteristics:

Fall-time:	.0375 sec.
Overshoot:	10.3%
Steady-state error:	0
Number of oscillations:	1

In order to effect a significant reduction in the tracking error of the system due to transient disturbances, the transient characteristics of the representing function were arbitrarily chosen as follows:

Fall-time:	Decrease by 300% to 500%.
Overshoot:	No increase over that of basic system.
Steady-state error:	Small.
Oscillations:	Essentially the same as for basic system.

The procedure followed in using the root-locus method was to choose a G_2 which would effect an increase of $W_n(G_1)$, the natural frequency of the basic system, by an amount of 300% to 500%. At the same time, the real roots of the basic system were compensated in such a way as to minimize the residues of the real roots of the resulting representing function (R.F.). Having done this, the R.F. approximated a second order system and its time response was generally known.

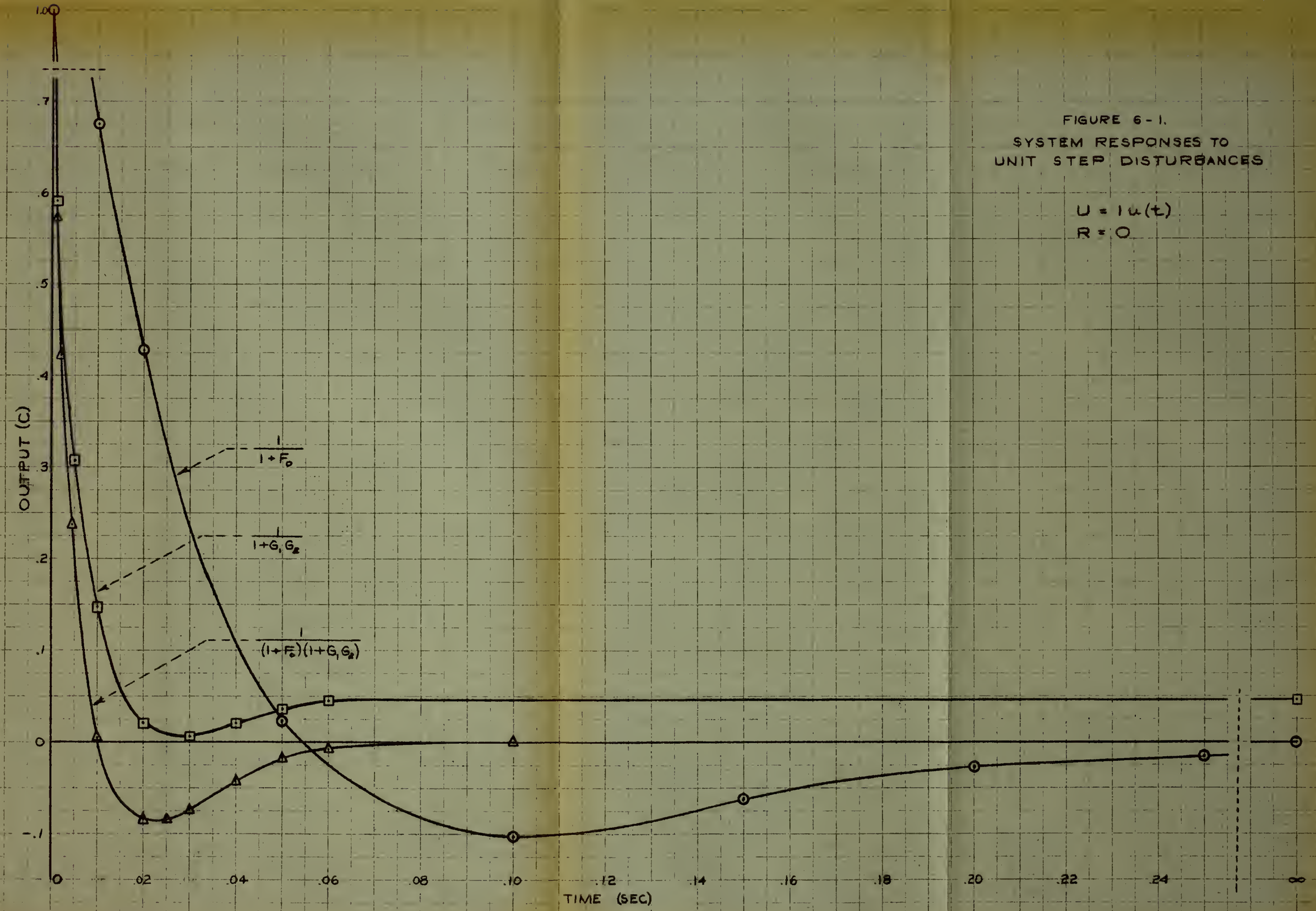

FIGURE 6-1.
SYSTEM RESPONSES TO
UNIT STEP DISTURBANCES

$U = 1u(t)$
$R = 0$

The simple correlations developed in Section 5 would then predict the desired function response.

The basic system closed-loop transfer function (G_1), was given in Section 3 as,

$$G_1 = \frac{37(s + 1.7)(s + 20)}{(s + 1.74)(s + 22.63 + j14.53)(s + 22.63 - j14.53)} ,$$

therefore,

$$\frac{1}{1+G_1G_2} = \frac{(s+1.74)(s+22.63+j14.55)(s+22.63-j14.55)\ D_2}{(s+1.74)(s+22.63+j14.55)(s+22.63-j14.55)\ D_2 + \ldots} \ldots$$

$$\ldots \overline{+\ 37(s+1.7)(s+20)\ N_2} , \qquad (6\text{-}1)$$

where $G_2 = \frac{N_2}{D_2}$.

Several values of G_2 were utilized in an attempt to meet the time response requirements arbitrarily chosen for R.F. The following are representative of the compensations attempted.

$\frac{K}{(s+a)}$ . . . . , a lag function,

$\frac{K(s+b)}{(s+a)}$ . . . . , b > a, a lag function,

$\frac{K(s+b)}{(s+a)}$ . . . . , a > b, a lead function,

Ks . . . . . , a derivative function.

The G_2 compensation which gave the desired position of the roots of the representing function (R.F.) was,

$$G_2 = \frac{21.06(s+96)(s+200)}{(s+20)(s+1000)} ,$$

a lag-lead compensating function. Fig. 6-2 shows the root-

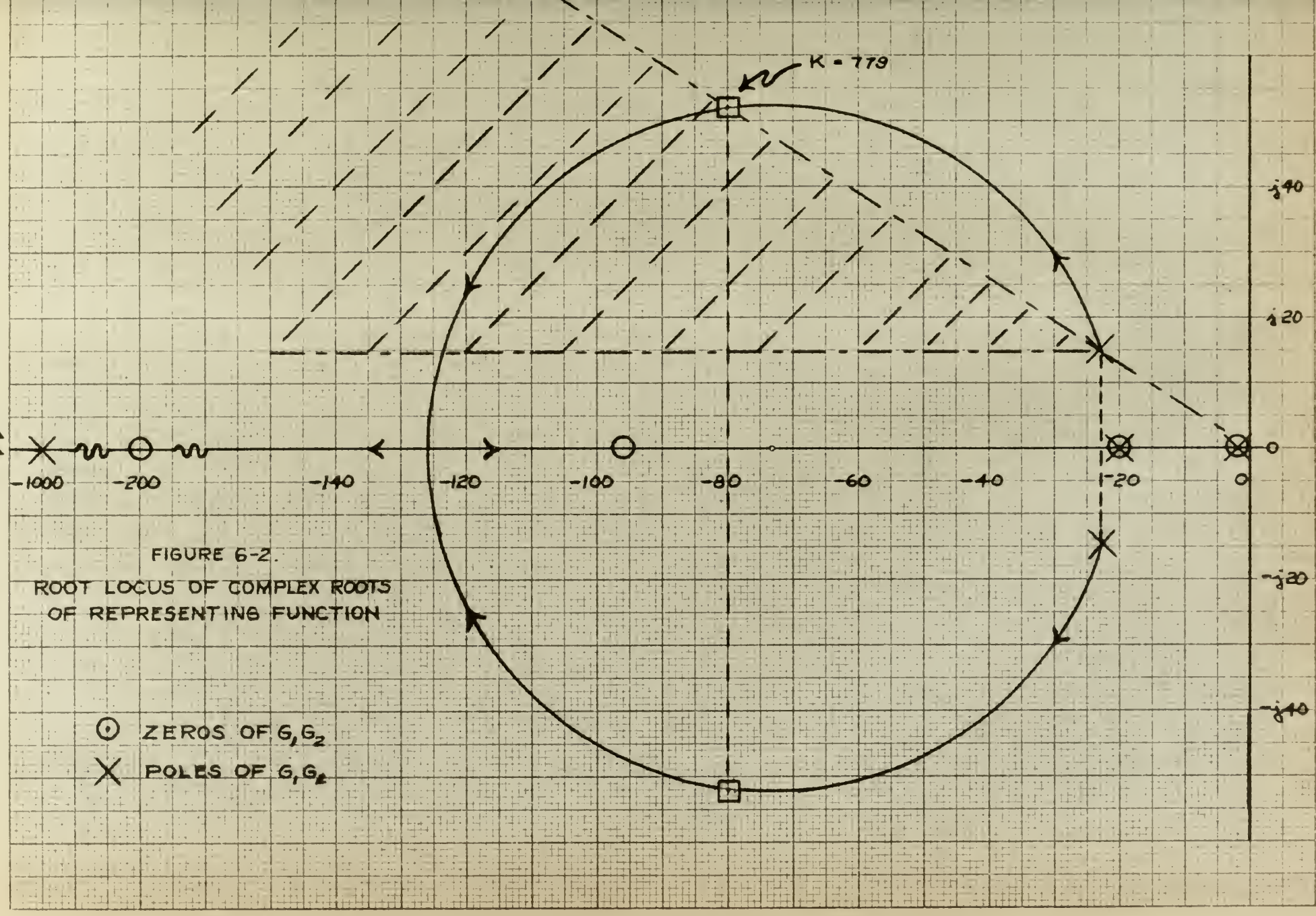

FIGURE 6-2.
ROOT LOCUS OF COMPLEX ROOTS OF REPRESENTING FUNCTION

locus of the complex roots of the R.F. utilizing this G_2. The complex roots are shown at

$$s_1 = -80-j52 \; ; \; s_2 = -80+j52.$$

The real roots of R.F. were solved numerically and were found to be:

$$s_3 = -1.712 \; ; \; s_4 = -20 \; ; \; s_5 = -1660 \; .$$

The natural frequency of the basic system, $W_n(G_1)$, is 26.9 rad. per sec. The natural frequency for R.F., $W_n(R.F.)$, is 95.35 rad. per sec. This is an increase of 350% over $W_n(G_1)$.

Section 5 has shown the form of the representing function to be $C_1 + C_2e^{-80t} \sin(52t + \Psi)$ for the complex roots of R.F. determined above. The phase angle (Ψ) lies in the second quadrant since the complex poles are located in the area that insures a phase angle in the second quadrant. The steady-state error constant (C_1) was approximated using equation (5-11) to be .079. Since the roots of this function are the same as those of the desired function, the latter function, to a second order approximation, takes the form, $C_3e^{-80t} \sin(52t + \Psi + \gamma)$.

In order to apply equation (5-8) for determining the phase difference (γ), the poles of F_o, G_1, and the complex poles of R.F. were plotted in Fig. 6-3 and γ was measured as +13 degrees.

The R.F., to a second order approximation, should give a fall-time of about 350% faster than that of the basic system, or applying equation (5-12),

$$\text{Fall-time (R.F.)} = \frac{26.9 \text{ rad/sec}}{95.35 \text{ rad/sec}} \times 0.0375 \text{ sec} = .01 \text{ sec.}$$

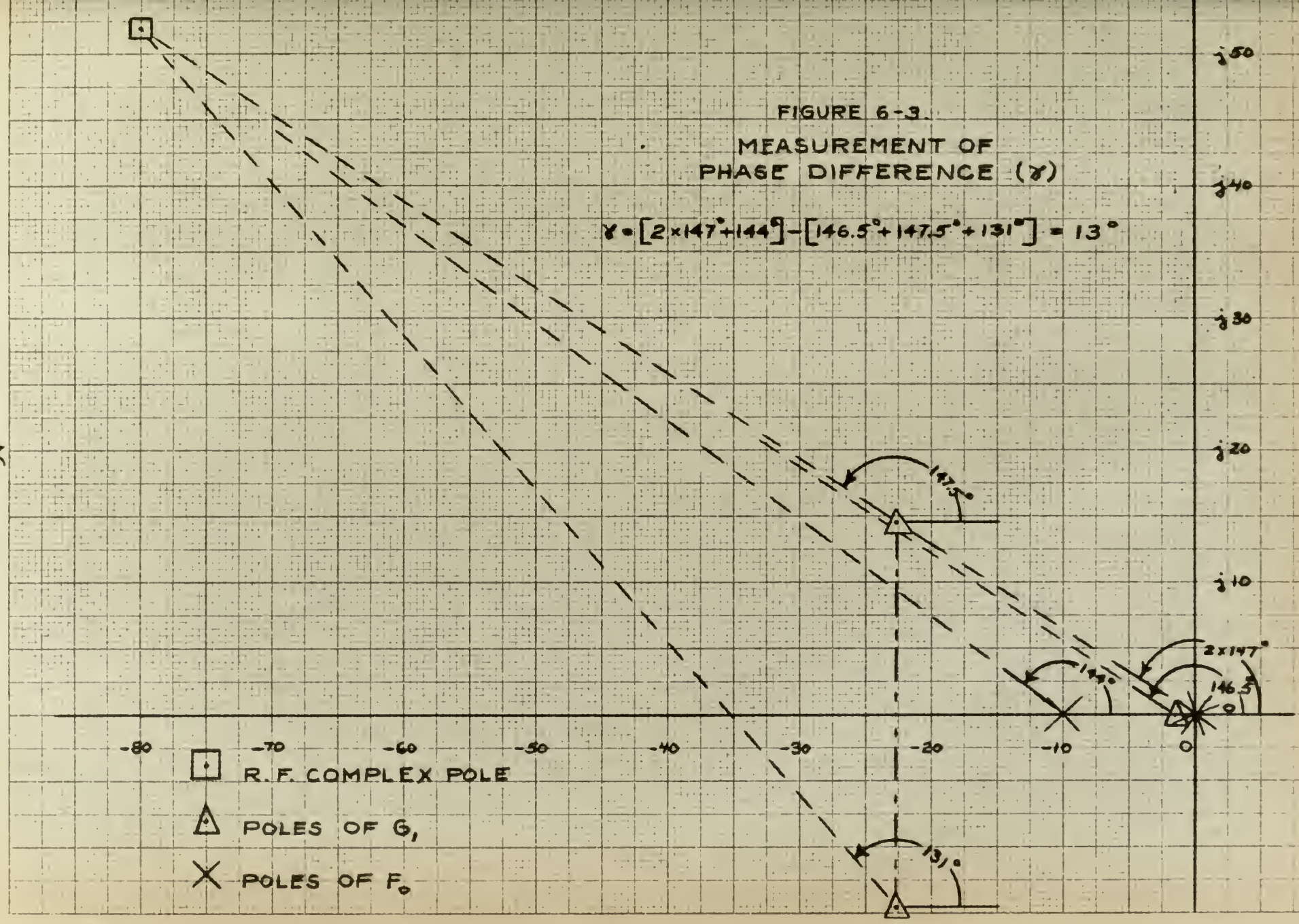

FIGURE 6-3.
MEASUREMENT OF
PHASE DIFFERENCE (γ)

$$\gamma = [2\times147^\circ+144^\circ]-[146.5^\circ+147.5^\circ+131^\circ] = 13^\circ$$

Since γ is positive and a relatively small angle, it is expected that the fall-time of the desired function response will be slightly less than that estimated for the R.F., that is, slightly less than .01 sec.

The overshoot of the R.F., to a second order approximation, was 0.008 . This value added to the C_1 of 0.079 gives a first prediction of desired function overshoot equal to 8.7% . Since γ was found to be positive, the overshoot of the desired response should be increased to some value slightly greater than that of the first prediction of desired function overshoot, that is, slightly greater than 8.7% . Thus, the predicted response of the desired function falls within the parameters selected for the new compensated system.

The desired transfer function is,

$$\frac{1}{(1+F_o)(1+G_1G_2)} = \frac{D_o}{(D_o+N_o)} \quad \frac{D_2(D_o+N_o)}{(D_oD_2 + N_oD_2 + N_oN_2)}$$

The roots, $(D_oD_2 + N_oD_2 + N_oN_2)$, have been found to be,

$$(s+1.712)(s+20)(s+1660)(s+80+j52)(s+80-j52).$$

Therefore, the desired transfer function is,

$$\frac{s^2(s+1.74)(s+10)(s+20)(s+1000)(s+22.63+j14.55)}{(s+1.74)(s+1.712)(s+20)(s+22.63+j14.55)(s+22.63-j14.55)} \times$$

$$\times \frac{(s+22.63-j14.55)}{(s+80+j52)(s+80-j52)(s+1660)} ,$$

which after simplification is,

$$\frac{s^2(s+10)(s+1000)}{(s+1.712)(s+1660)(s+80+j52)(s+80-j52)} . \qquad (6\text{-}2)$$

Using the graphical residue method on equation (6-2), the output due to a load disturbance applied as a unit step is,

$$C = .990e^{-80t}\sin(52t + 2.530) - .000965e^{-1.712t} + 0.437e^{-1660t} .$$

Fig. 6-1 shows a plot of this response. The predicted response characteristics together with those obtained from Fig. 6-1 are as follows:

	Predicted	Actual
Fall-time:	< .01 sec	.007 sec
Overshoot:	8.7% +	8.6%
Steady-state error:	0	0
Oscillations:	--	1

The fall-time has been increased by 535% over that of the basic uncompensated system response. The overshoot has been decreased by 16.5% and no steady-state error results. This improvement in the regulation response did not result in any change in the desired original input-output response of the basic system.

In order to check the accuracy of the correlation technique rules developed, the response of the representing function to a unit step input was determined using graphical residue methods, and was found to be,

$$C_{(R.F.)} = .0488 + .709e^{-80t}\sin(52t + 2.308) + .000745e^{-1.712t} + .426e^{-1660t} .$$

Fig. 6-1 shows a plot of this R. F. response. The difference in phase angles between the R. F. and the desired function is equal to (2.530-2.308) radians. Thus, the true value of γ is equal to 0.222 radians or 12.7 degrees. The γ obtained through the correlation rule, equation (5-8), was 13 degrees. The estimate of the R. F. C_1 was .079, while the actual value of C_1 was computed to be .0488. The accuracy of the correlation rules used in the representing function technique has been shown to be more than sufficient. The time saved in using this technique for determining the desired conditional feedback compensation was considerable.

7. Selection of disturbance input.

The external load torque on the antenna due to wind gusting is a function of time with three independent variables, wind velocity, wind direction, and the tracking direction of the antenna. To evaluate the compensation, it is desirable to investigate its effectiveness in reducing the greatest expected disturbance error. Since the three variables affecting the disturbance output are independent, the maximum error will occur when the errors due to each variable are maximum.

To investigate the effectiveness of the compensation, a wind velocity profile having the greatest expected severity was used. From consideration of data pertaining to wind gust velocities[2], a representative velocity profile was developed which would produce the maximum expected disturbance error. This velocity profile is shown in Fig. 7-1. A steady 25 miles per hour wind was assumed to exist prior to the gust. The wind velocity then increased smoothly to a peak of 60 miles per hour in one-half second and remained at this value for one-half second. The maximum gust velocity normally decreases at a slower rate than it increases during the gust build-up. Since only that part of the gust profile resulting in the largest disturbance error is of interest, the trailing edge of the actual gust profile need not be considered.

[2]W. R. Gregg, Aeronautical Meteorology, pp. 269-274, 1930

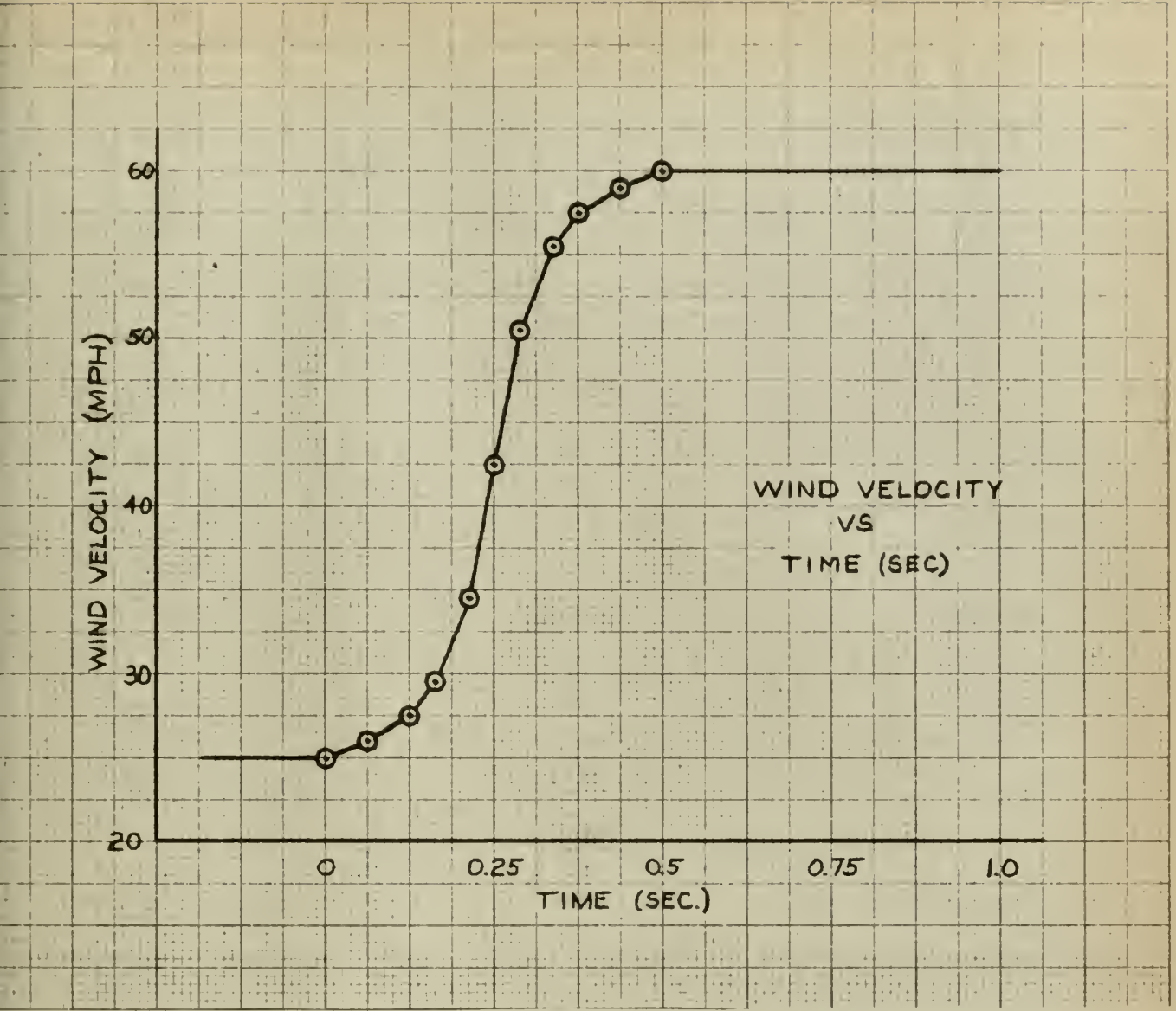

Note: The wind velocity profile was developed as straight line segments approximating a smoothly increasing wind gust in order to utilize a function generator in simulating the wind velocity input to the analog computer simulation described in Appendix IV.

Figure 7-1. Representative wind velocity profile.

The true wind direction was considered constant since wind direction changes are most likely to be negligible during the short interval of the gust being used. Since true wind has been considered constant during the one-half second of applied gusting, the change in relative wind direction is a function only of antenna rotation. The targets tracked by this antenna are earth-orbiting satellites which require relatively slow tracking rates. Thus, the change in relative wind due to antenna rotation is negligible during the one-half second gusting interval. During the gust, the antenna was considered to be in that position, relative to the true wind, which would cause the greatest disturbance torque for any given wind velocity.

A plot of wind moment coefficient (C_{mg}) about the antenna gimbal center vs. angle of wind incidence has been prepared for the given antenna from wind tunnel tests made on a 1/30th scale model.[3] The data is reproduced in Fig. 7-2. The use of a "spoiler," fixed to the back side of the antenna around the periphery of the dish, was used to reduce maximum torque loading on the antenna by approximately 50 percent.

The moment about the antenna gimbal center (M_g) was derived in Appendix III as

$$M_g = 201.9\, C_{mg} V_w^2 \quad \text{(lb-ft)} , \qquad (7\text{-}1)$$

[3]Guggenheim Aeronautical Laboratory, California Institute of Technology, Report 737, 1960.

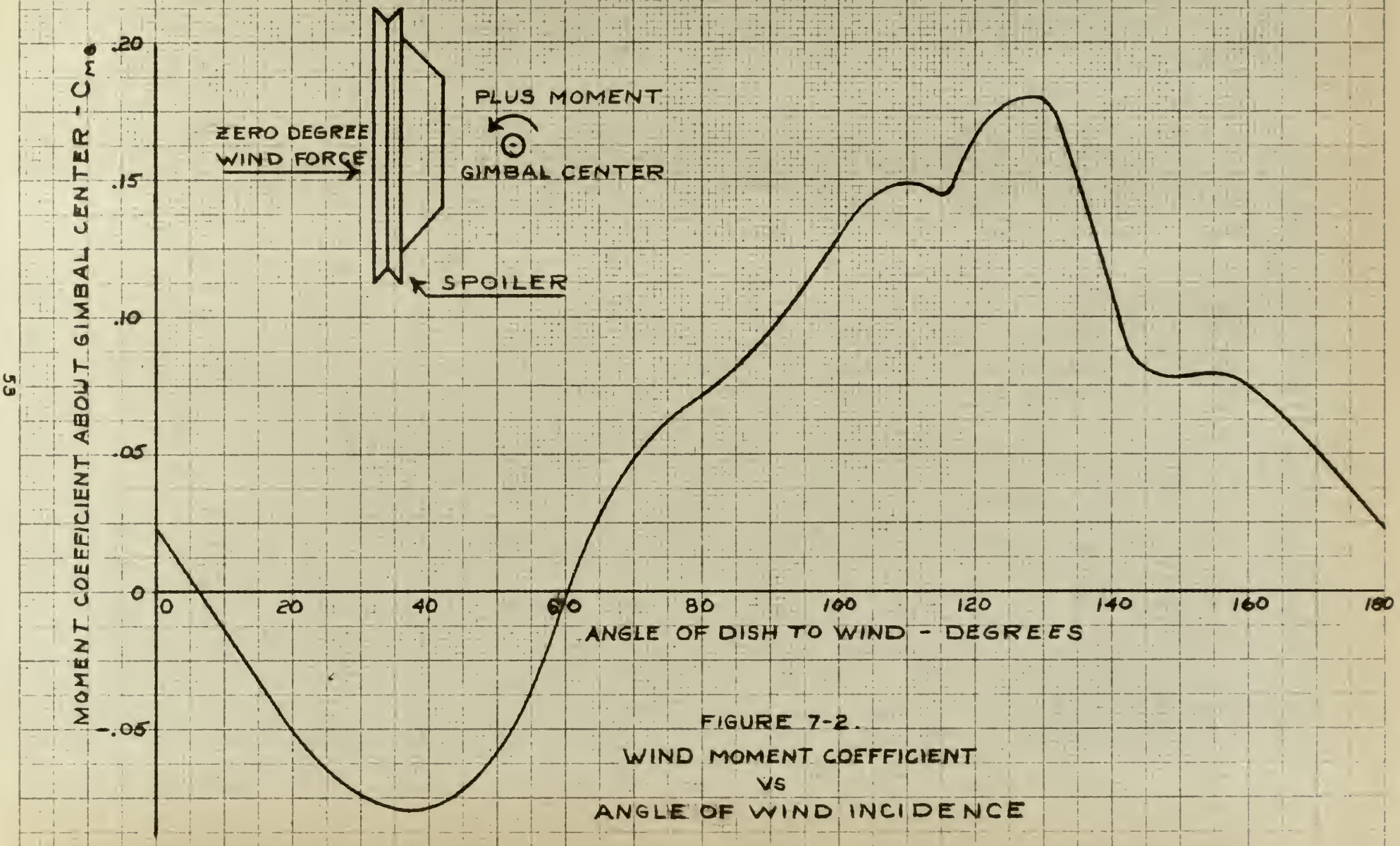

FIGURE 7-2.
WIND MOMENT COEFFICIENT
VS
ANGLE OF WIND INCIDENCE

where C_{mg} = dimensionless moment coefficient about gimbal center

V_w = wind velocity (ft/sec).

For a maximum velocity of 60 MPH and a maximum C_{mg} of 0.189 (130^{o} angle of wind incidence), the maximum M_g computed from equation (7-1) is 137.3×10^{3} lb-ft. This moment, M_g, is the external torque (T_e) applied to the output azimuth drive shaft.

8. Evaluation of the conditional feedback compensation.

The evaluation of the designed conditional feedback compensation is made on the basis of a comparison between the uncompensated disturbance-output response and the compensated system response.

A step position disturbance input was used in Section 6 to determine the design of the compensation since this input represented the most severe disturbance, though only theoretically possible. The compensation was designed to provide for an arbitrarily selected improvement in system response. These responses were shown in Fig. 6-1.

A comparison of system response to a step velocity disturbance input was made to closer approximate the system response to wind gusting. These responses are shown in Fig. 8-1.

In order to verify the degree of response improvement indicated as a result of the above two disturbance inputs, the system response to the wind gust profile of Fig. 7-1 was obtained. The electronic analog computer simulation for this disturbance input was formulated in Appendix III. Appendix IV presents the analog simulation used to determine the system response to the wind gust. Both compensated and uncompensated system responses to the gust profile of Fig. 7-1 are shown in Fig. 8-2a.

In order to note the system response to a wind gust more severe than that derived in Section 7, and, in addition, one of less severity, wind gust profiles of one-half and

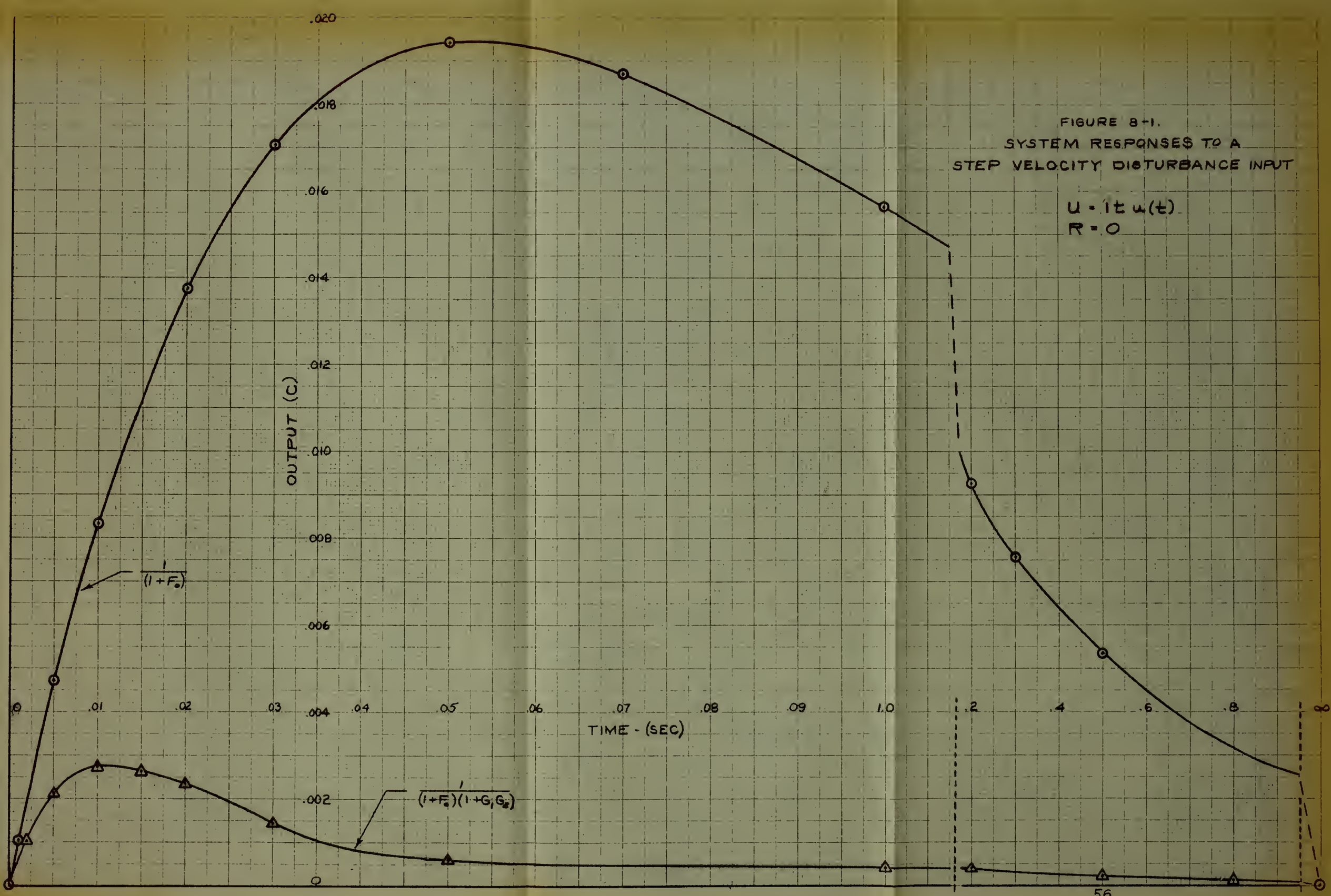

FIGURE 8-1.
SYSTEM RESPONSES TO A
STEP VELOCITY DISTURBANCE INPUT

$U = 1t\,u(t)$
$R = 0$

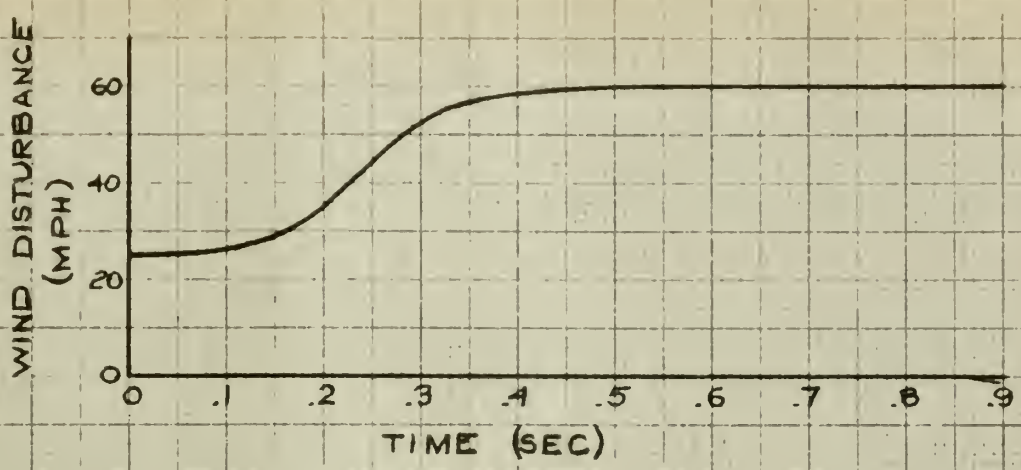

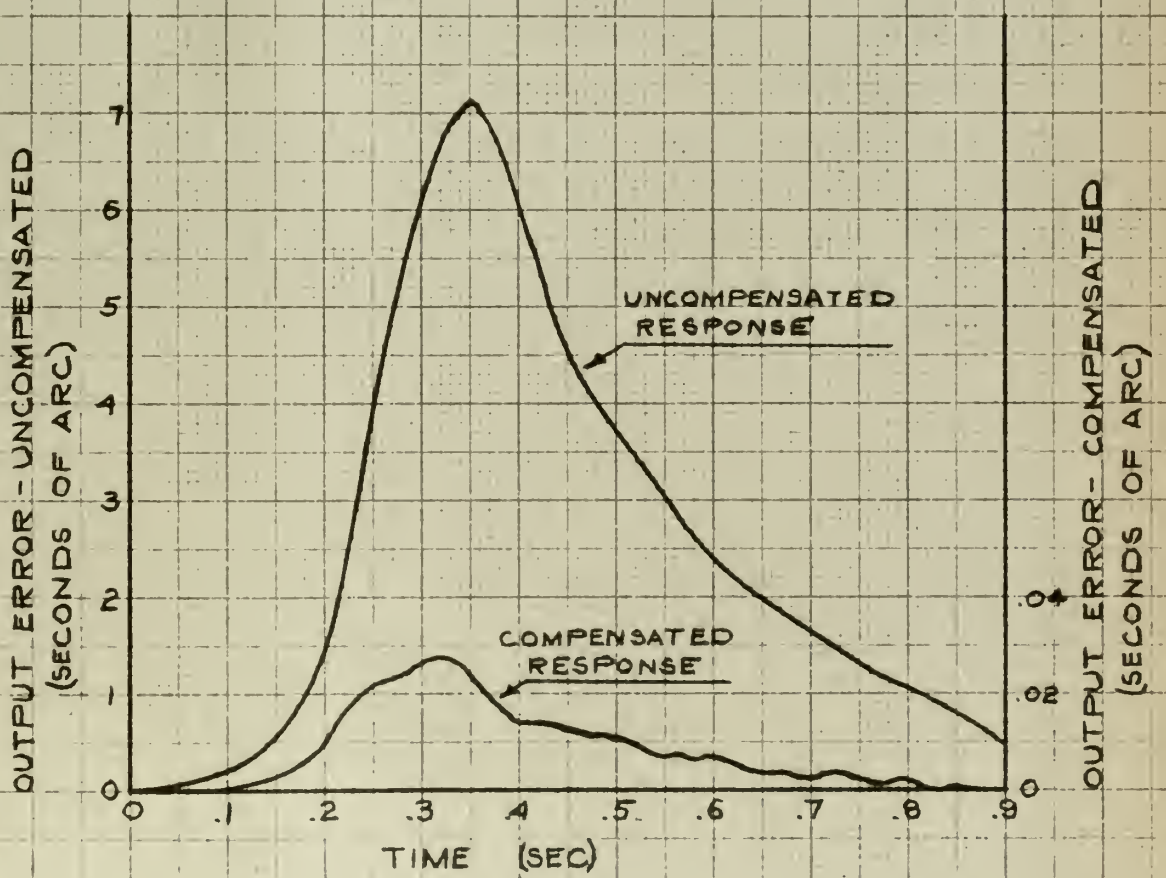

FIGURE 8-2a. WIND GUST DISTURBANCE RESPONSE. (.5 SEC. INTERVAL)

twice the time interval of the profile of Fig. 7-1 were applied. These responses are shown in Fig. 8-2b and Fig. 8-2c. The frequency response curves for the compensated system are shown in Fig. 8-3.

Table I shows the disturbance response characteristics of the uncompensated and compensated systems for the disturbance inputs applied. The most significant parameter upon which to evaluate the compensated system is the maximum error caused by the wind gust. Table I shows this error, due to the wind gust of Fig. 7-1, to be 7.2 seconds of arc for the uncompensated system. With the addition of the conditional feedback compensation, this error was reduced to 0.028 seconds of arc. It is emphasized that this substantial reduction in antenna position error due to wind loading has been effected without change to the original input-output response.

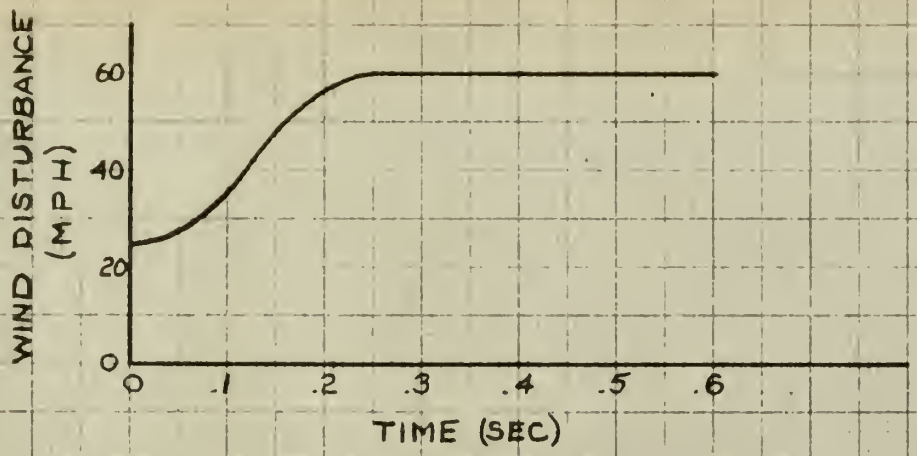

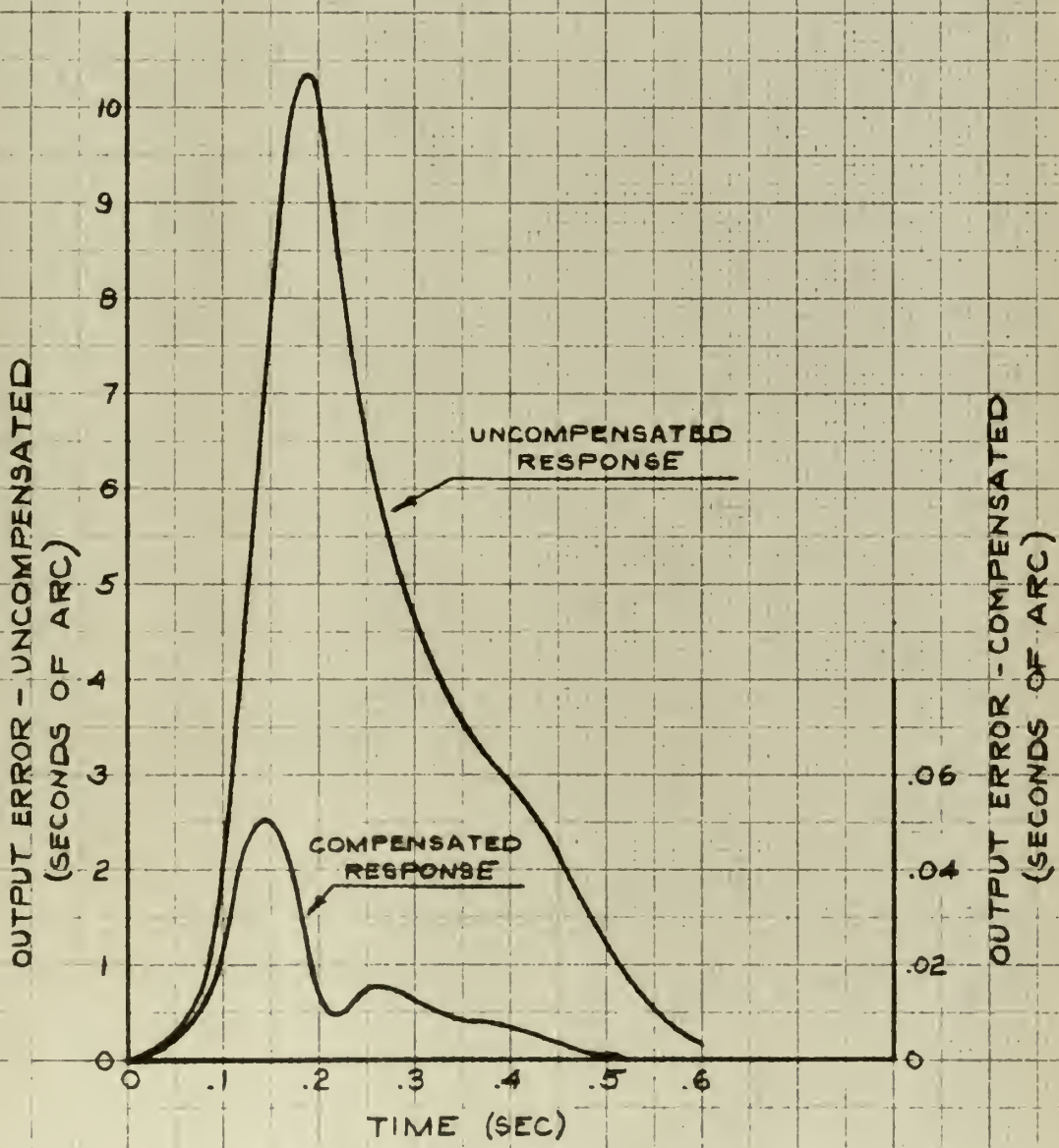

FIGURE B-2b. WIND GUST DISTURBANCE RESPONSE (.25 SEC. INTERVAL)

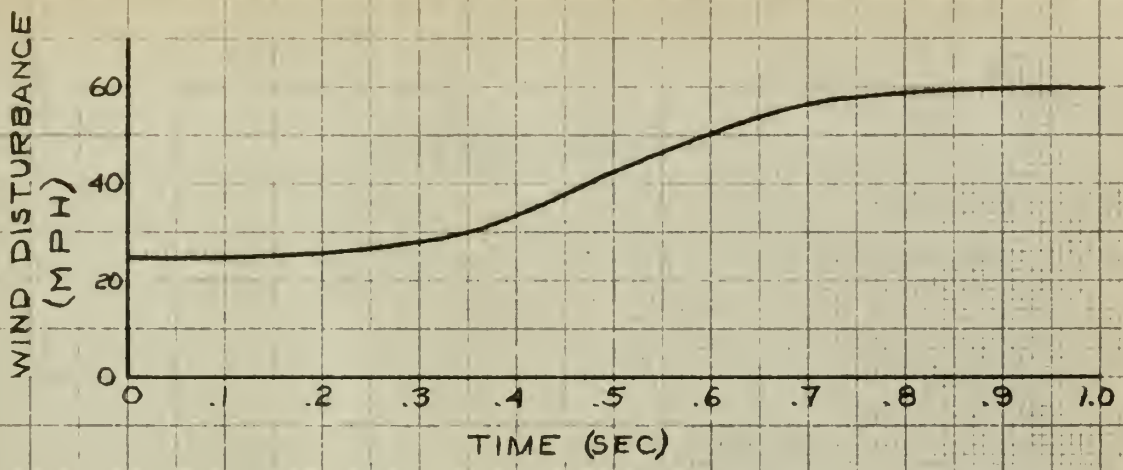

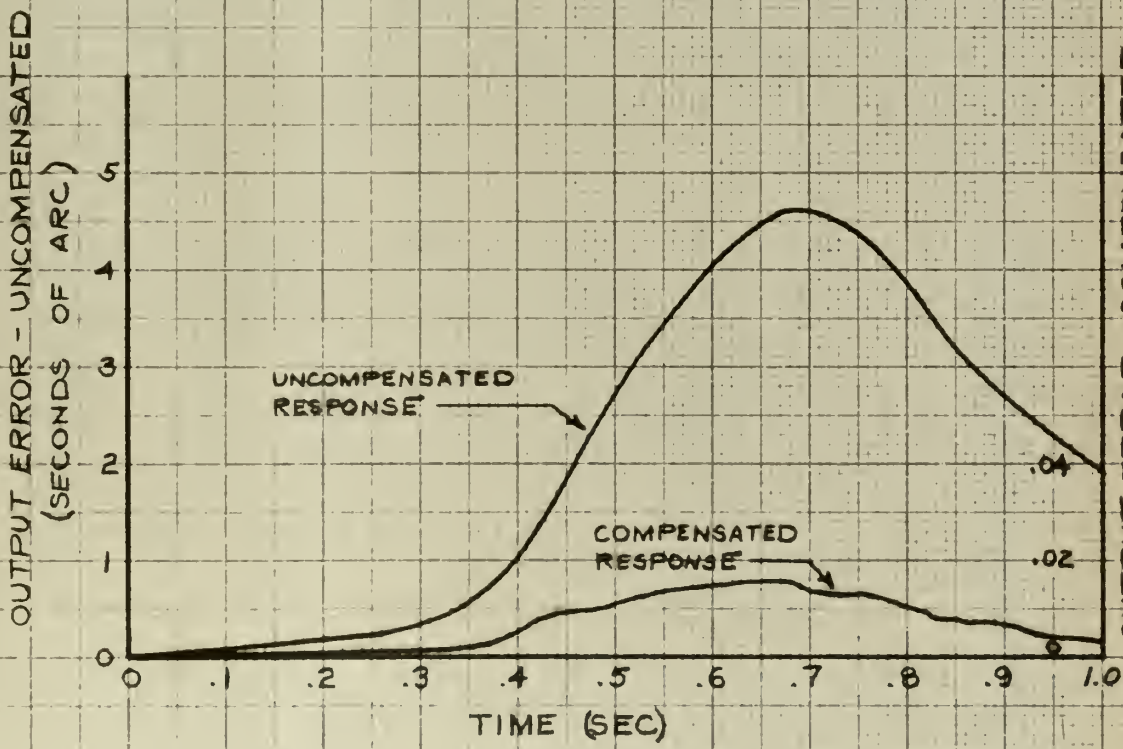

FIGURE 8-2.c. WIND GUST DISTURBANCE RESPONSE
(1 SEC. INTERVAL)

FIGURE 8-3.

DISTURBANCE - OUTPUT FREQUENCY RESPONSE OF COMPENSATED SYSTEM

$$\frac{C}{U} = \left(\frac{1}{1+F_o}\right)\left(\frac{1}{1+G_1G_2}\right)$$

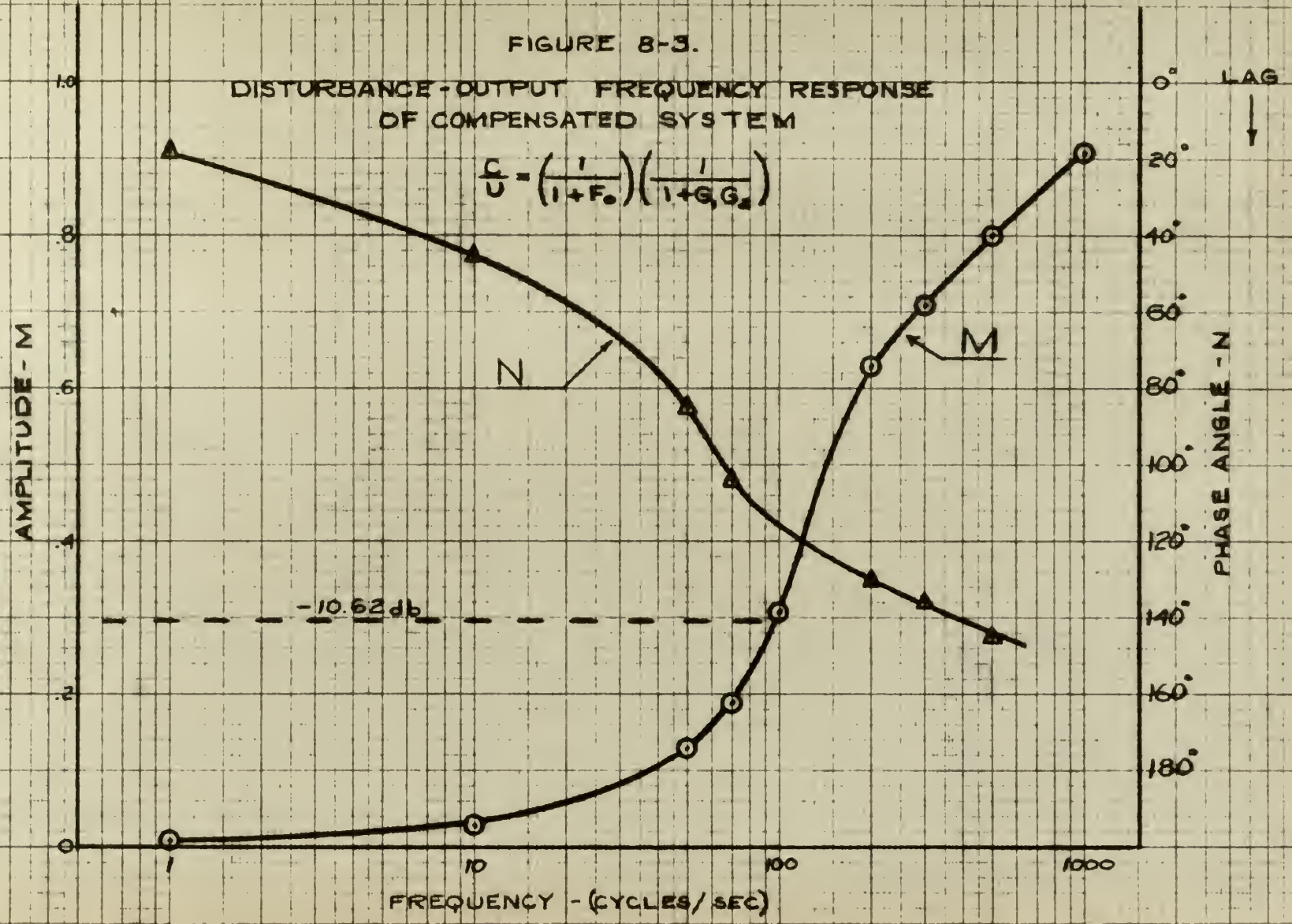

TABLE I

DISTURBANCE RESPONSE CHARACTERISTICS

Comparison Parameters	Step Position		Unit Sec. Step Velocity		Simulated Wind					
	Fig. 6-1		Fig. 8-1		Fig. 8-2a		Fig. 8-2b		Fig. 8-2c	
	Un-Comp.	Comp.	Un-Comp.	Comp.	Un-Comp.	Comp.	Un-Comp.	Comp.	Un-Comp.	Comp.
Overshoot (%)/Max. Error (Sec. of Arc)	10.3%	8.6%	.0194	.0028	7.20	.028	10.3	.051	4.7	.017
Time to Maximum Error (Sec.)	.10	.023	.051	.011	.35	.32	.18	.14	.70	.63
Steady-State Error	0	0	0	0						
Fall Time (Sec.)	.0375	.007								
Settle-Out Time (Sec.)-5% Level	.17	.038								

	Fig. 4-6 Uncomp.	Fig. 8-3 Comp.
Bandwidth (C.P.S.)	2.10	98
Phase Shift (Degrees)	-78.0	-113

9. Conclusions.

This study has shown that there exists a compensation technique which can be successfully utilized to reduce antenna tracking errors due to wind disturbances without effecting a change in tracking input-output response.

Section 2 introduced the conditional feedback compensation method and has shown that this method permits design specifications on disturbance-output response to be met without change to the tracking input-output response. A specific conditional feedback compensation was developed to obtain a substantial degree of reduction of wind disturbance tracking error. The degree of disturbance error reduction is presented in Table I of Section 8. The representative wind velocity profile developed in Section 7 was applied as the disturbance input, and the resulting error decreased from 7.2 seconds of arc without compensation to .028 seconds of arc with conditional feedback compensation. This represents a 257:1 reduction in disturbance error. In addition, this substantial error reduction was achieved with a faster response time. The response improvement of the compensated system is made more evident by noting that the other response parameters listed in Table I show substantial improvement over the uncompensated system. A significant disturbance error reduction might be expected when it is noted that bandwidth has been increased from 2 cps. to 98 cps.

In order to determine the system response due to any given conditional feedback compensator, two root locus plots would have been required to place the roots of the closed loop

function. It was anticipated that several values of compensation would have to be investigated before a satisfactory compensator could be obtained. The representing function technique was originated for the purpose of expediting the above repetitive process. This technique was employed in the determination of the desired compensator. The representing function technique proved to be accurate, expeditious, and simple to apply. A step-by-step procedure for its application is given at the conclusion of Section 5.

BIBLIOGRAPHY

1. G. Lang and J. M. Ham, Conditional Feedback Systems - A New Approach to Feedback Control, A.I.E.E. (A&I), pp. 152-158, July 1955.

2. G. S. Brown and D. P. Campbell, Principles of Servomechanisms, John Wiley & Sons, 1948.

3. J. G. Truxal, Automatic Feedback Control Synthesis, McGraw-Hill Company, 1955.

4. H. Chestnut and R. W. Mayer, Servomechanisms and Regulating System Design, Vol. I, John Wiley & Sons, 1951.

5. R. A. Burn and R. M. Saunders, Analysis of Feedback Control Systems, McGraw-Hill Company, 1955.

6. G. C. Newton, Jr., Analytic Design of Linear Feedback Controls, John Wiley & Sons, 1957.

7. F. E. Nixon, Principles of Automatic Controls, Prentice-Hall, 1953.

8. J. E. Gibson, How to Specify the Performance of Closed-loop Systems, Control Eng., pp. 122-129, Sept. 1956.

9. R. C. H. Wheeler, Basic Theory of the Electronic Analog Computer, Donner Scientific Co., 1955.

APPENDIX I

COMPLEX ZERO COMPENSATOR

An electronic compensator, Fig. I-1, has been developed,[4] utilizing an operational amplifier, which will essentially cancel the complex poles of a cascaded transfer function.

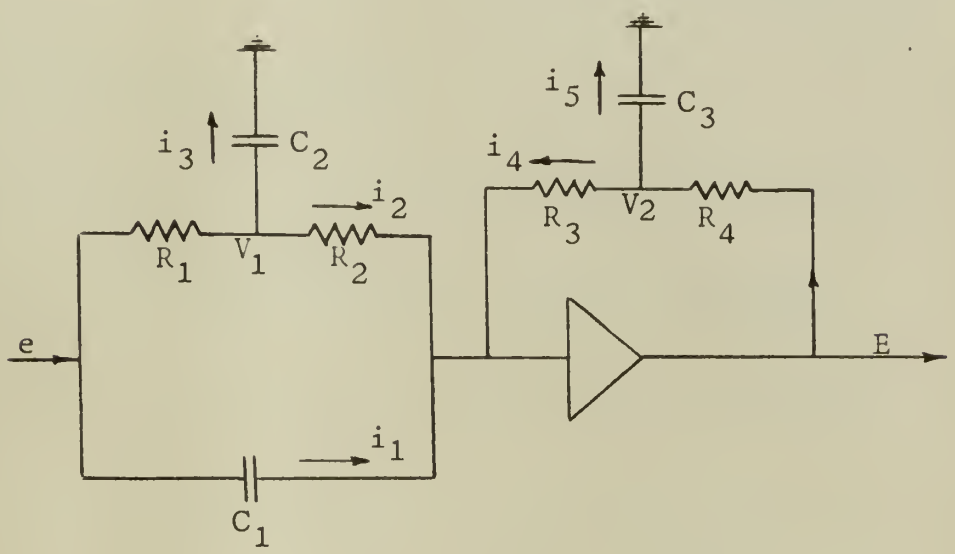

Figure I-1. Complex zero compensator schematic.

$$i_1 + i_2 + i_4 = 0 \qquad \text{(I-1)}$$

$$i_1 = C_1 e s \qquad \text{(I-2)}$$

$$i_2 = \frac{V_1}{R_2}$$

$$\frac{e - V_1}{R_1} = i_2 + i_3$$

$$i_3 = C_2 V_1 s$$

$$\frac{e}{} = V_1\left(\frac{1}{R_1} + \frac{1}{R_2} + C_2 s\right)$$

$$V_1 = \frac{eR_2}{R_1 + R_2 + R_1 R_2 C_2 s}$$

$$i_2 = \frac{e}{R_1 + R_2 + R_1 R_2 C_2 s} \qquad \text{(I-3)}$$

[4] G. A. Korn and T. M. Korn, Electronic Analog Computers, pp. 417-420, McGraw-Hill Co., 1956

$$i_4 = \frac{V_2}{R_3} \qquad \frac{E - V_2}{R_4} = i_4 + i_5$$

$$i_5 = C_3 V_2 s$$

$$\frac{E}{R_4} = V_2\left(\frac{1}{R_3} + \frac{1}{R_4} + C_3 s\right)$$

$$V_2 = \frac{ER_3}{R_3 + R_4 + R_3R_4C_3s}$$

$$i_4 = \frac{E}{R_3 + R_4 + R_3R_4C_3s} \tag{I-4}$$

Substituting (I-2), (I-3), and (I-4) into (I-1) gives

$$C_1 es + \frac{e}{R_1 + R_2 + R_1R_2C_2s} + \frac{E}{R_3 + R_4 + R_3R_4C_3s} = 0 . \tag{I-5}$$

Letting $R_1 = R_2 = R_3 = R_4 = 1$ megohm, then equation (I-5) becomes

$$C_1 es + \frac{e}{2x10^6 + C_2 s x10^{12}} + \frac{E}{2x10^6 + C_3 s x10^{12}} = 0 \tag{I-6}$$

$$\frac{e\,(2x10^6 C_1 s + C_1C_2 s^2 x10^{12} + 1)}{2x10^6 + C_2 s x10^{12}} = \frac{-E}{2x10^6 + C_3 s x10^{12}} \tag{I-7}$$

If C_2 is made equal to C_3, the denominators of (I-7) become equal, and (I-7) reduces to

$$\frac{E}{e} = -C_1C_2x10^{12}\left(s^2 + \frac{2}{C_2x10^6}\, s + \frac{1}{C_1C_2x10^{12}}\right) . \tag{I-8}$$

If the capacitors are valued in micro-farads, equation (I-8) becomes

$$\frac{E}{e} = -C_1C_2\left(s^2 + \frac{2}{C_2}\, s + \frac{1}{C_1C_2}\right) . \tag{I-9}$$

Equation (I-9) is of the form of a constant times a complex zero, where C_1 and C_2 are picked so that the coefficients in this equation equal those of the complex poles it is to cancel.

Depending on the values of capacitors used, it may be necessary to modify the circuit values slightly to suppress high frequency oscillations in the compensator amplifier. Reduction of the value of C_3 or placing a relatively small resistance (about 0.1 megohms) between C_3 and ground has been found effective. Such changes naturally reduce the cancellation effectiveness of the compensator, but to a degree generally within acceptable limits.

APPENDIX II

GRAPHICAL RESIDUE TECHNIQUE FOR DETERMINING THE TRANSIENT RESPONSE EQUATION OF A SYSTEM

Consider the disturbance-output transfer function of the uncompensated basic system:

$$\frac{C}{U} = \frac{1}{1 + F_o} = \frac{s^2(s + 10)}{(s + 1.74)(s + 22.63 - j14.55)} \times$$

$$\times \frac{1}{(s + 22.63 + j14.55)} . \qquad \text{(II-1)}$$

Let $U(t) = A\,u(t)$, where $A = 1$. Therefore $U(s) = \frac{1}{s}$, and equation (II-1) becomes

$$C = \frac{s(s + 10)}{(s + 1.74)(s + 22.63 - j14.55)(s + 22.63 + j14.55)} . \qquad \text{(II-2)}$$

The poles and zeros of equation (II-2) are plotted in Fig. II-1. The residue at (-1.74) is equal to

$$\frac{\prod(\text{ vectors from the zeros to the pole }) \; e^{(\text{pole})t}}{\prod(\text{ vectors from the remaining poles to the pole})}$$

or,

$$\frac{(r_1 - z_1)(r_2 - z_2)}{\left[r_1 - (\alpha + jw_c)\right]\left[r_1 - (\alpha - jw_c)\right]} \; e^{r_1 t} . \qquad \text{(II-3)}$$

From Fig. II-1 equation (II-3) becomes

$$\frac{(1.74 \angle 180^\circ)(8.26 \angle 0^\circ)}{(25.45 \angle 2\pi - \theta_1)(25.45 \angle \theta_1)} \; e^{1.74 \angle 180^\circ t}$$

or,

$$-0.0222\, e^{-1.74\, t} . \qquad \text{(II-4)}$$

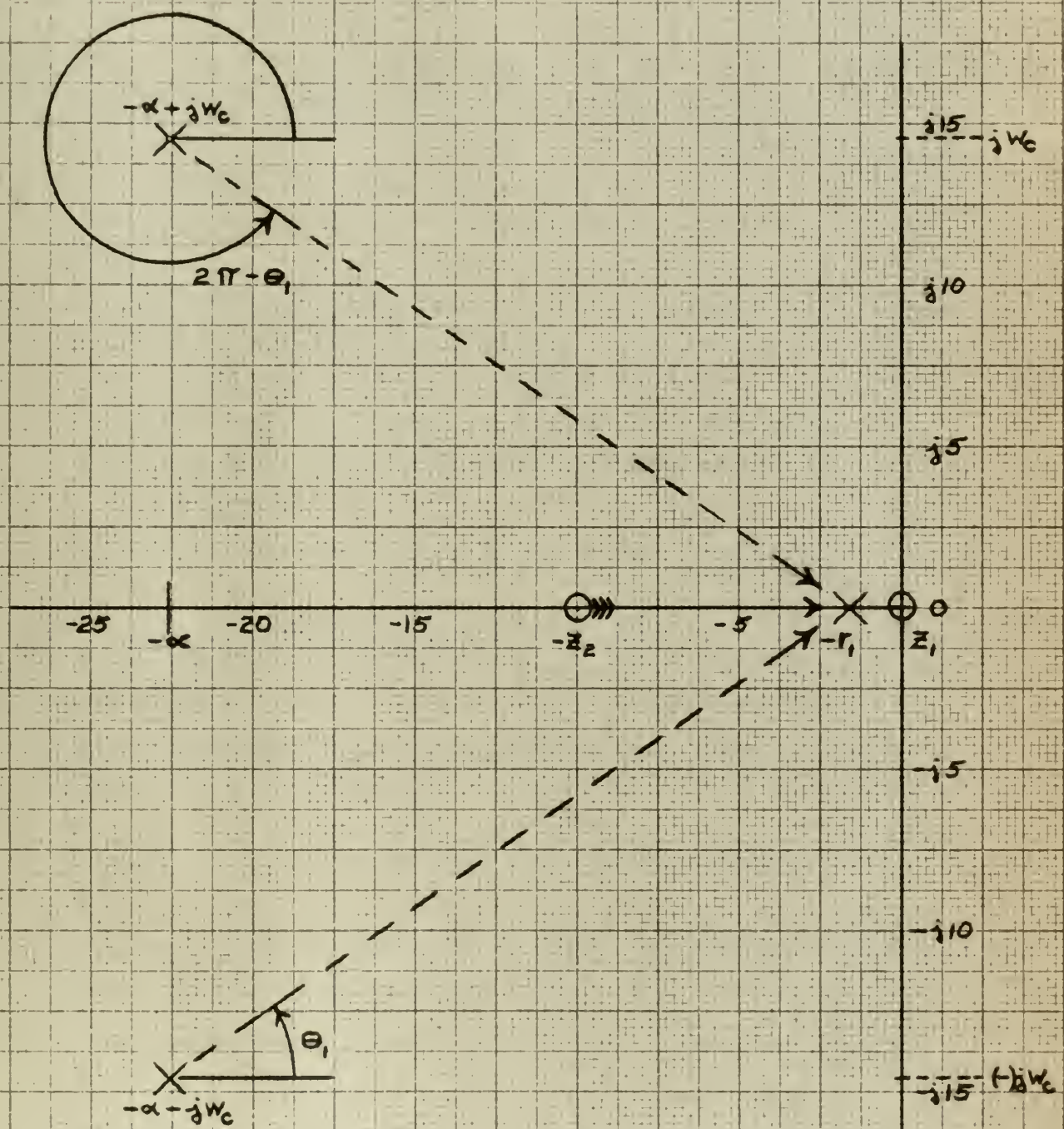

FIGURE II-1

POLE AND ZERO PLOT OF $\frac{1}{1+F_o}\,u(t)$ FOR DETERMINATION OF RESIDUE AT POLE (-1.74)

The residue at the complex pole (- 22.63 + j14.55) is equal to:

$$\frac{\left[(-\alpha + jw_c) - z_1\right]\left[(-\alpha + jw_c) - z_2\right]}{\left[(-\alpha + jw_c) - r_1\right]\left[(-\alpha + jw_c) - (-\alpha - jw_c)\right]} e^{(-\alpha + jw_c)t} \qquad \text{(II-5)}$$

From Fig. II-2, equation (II-4) becomes

$$= \frac{(26.9 \angle \Psi)(19.25 \angle \theta_2)}{(25.45 \angle \pi - \theta_1)(2 \times 14.55 \angle \theta_3)} e^{(-22.63 + j14.55)t}$$

$$= \frac{(26.9 \angle \Psi)(19.25 \angle \theta_2)}{(25.45 \angle \pi - \theta_1)(14.55)} \times \frac{e^{(-22.63 + j14.55)t}}{2j}$$

$$= 1.395\, e^{-22.63t} \sin(14.55t + \Psi + \theta_2 - \pi + \theta_1)$$

$$= 1.395\, e^{-22.63t} \sin(14.55t + 2.319)\,. \qquad \text{(II-6)}$$

Combining equations (II-6) and (II-4) yields the complete transient response equation for the system $\frac{1}{1 + F_o}\, u(t)$;

$$C = 1.395\, e^{-22.63t} \sin(14.55t + 2.319) - 0.0222\, e^{-1.74t}$$

By this same technique, the other disturbance-output transfer functions used in this thesis can be converted to their equivalent transient response equations for various input signals. A listing of these transient response equations for unit step and unit velocity inputs follows.

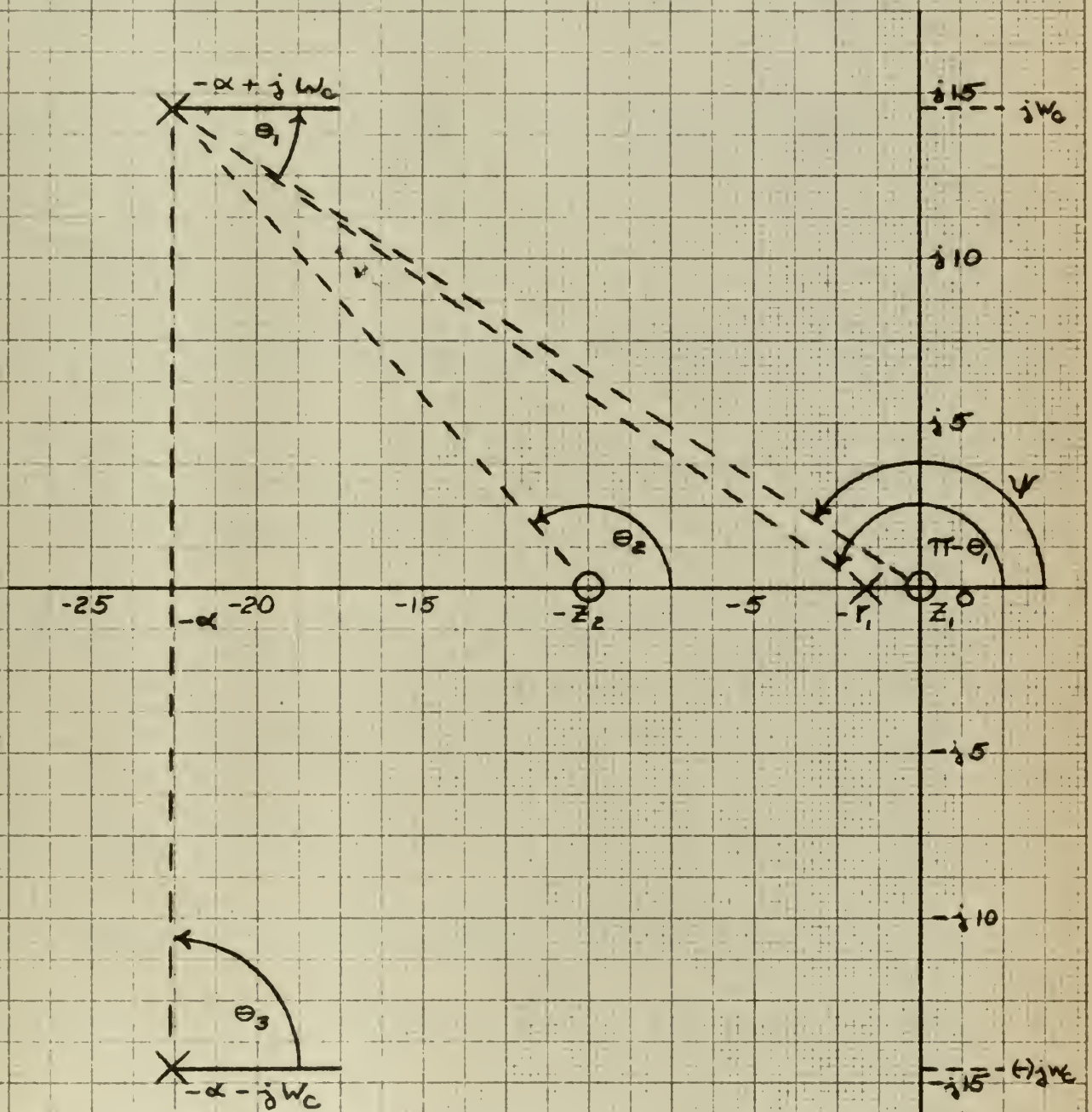

FIGURE II-2.

POLE AND ZERO PLOT OF $\frac{1}{1+F_o}u(t)$ FOR DETERMINATION OF RESIDUE AT POLE $(-22.63+j14.55)$

$$\frac{C}{U} = \frac{1}{1 + F_o} = \frac{s^2(s + 10)}{(s + 1.74)(s + 22.63 - j14.55)(s + 22.63 + j14.55)}$$

$$\frac{C(t)}{1u(t)} = 1.395\ e^{-22.63t} \sin(14.55t + 2.319) - 0.0222\ e^{-1.74t}$$

$$\frac{C(t)}{tu(t)} = 0.0520\ e^{-22.63t} \sin(14.55t - 0.247) + 0.0127\ e^{-1.74t}$$

- -

$$\frac{C}{U} = \frac{1}{1 + G_1G_2}$$

$$= \frac{(s + 1.74)(s + 22.63 - j14.55)(s + 22.63 + j14.55)(s + 1000)}{(s + 1.412)(s + 80 - j52)(s + 80 + j52)(s + 1660)}$$

$$\frac{C(t)}{1u(t)} = 0.0488 + 0.709\ e^{-80t} \sin(52t + 2.308) + .000745\ e^{-1.712t} + 0.426\ e^{-1660t}$$

$$\frac{C(t)}{tu(t)} = 0.00172 + 0.0488t + 0.00738\ e^{-80t} \sin(52t - 0.265) + 0.000423\ e^{-1.712t} - 0.000257\ e^{-1660t}$$

- -

$$\frac{C}{U} = \left[\frac{1}{1 + F_o}\right]\left[\frac{1}{1 + G_1G_2}\right]$$

$$= \frac{s^2(s + 10)(s + 1000)}{(s + 1.712)(s + 80 - j52)(s + 80 + j52)(s + 1660)}$$

$$\frac{C(t)}{1u(t)} = 0.990\ e^{-80t} \sin(52t + 2.530) - 0.000965\ e^{-1.712t} + 0.437\ e^{-1660t}$$

$$\frac{C(t)}{tu(t)} = 0.0104\ e^{-80t} \sin(52t - 0.0306) + 0.000564\ e^{-1.712t} - 0.000263\ e^{-1660t}$$

APPENDIX III

DEVELOPMENT OF DISTURBANCE TRANSFER FUNCTION

The purpose of this Appendix is to develop the relationship between the disturbance input (U), a function of the disturbing wind velocity (V_w), and the antenna position angle (Θ_L). The development of this transfer function was undertaken in two steps. First, the transfer equation of the disturbance torque (T_e) with respect to V_w was determined. The transfer function of T_e to the antenna position angle (Θ_L) was then determined and the two steps combined to give the transfer function of V_w to Θ_L.

Fig. 7-2 presents a plot of the non-dimensional moment coefficient (C_{mg}) of the antenna as a function of relative wind direction. Using Fig. 7-2 to determine C_{mg}, the moment about the antenna gimble center (M_g) which is also the external torque (T_e), was found as follows:[5]

$$T_e = M_g = C_{mg}\, q\, S\, r \qquad \text{(III-1)}$$

where, $q = \frac{1}{2} \rho V_w^2$, the dynamic pressure ($\frac{lb}{ft^2}$),

$S = 2830\ ft^2$, antenna dish frontal area,

ρ = air density ($\frac{lb\text{-}sec^2}{ft^4}$),

$r = 30$ ft, antenna dish radius.

The data of Fig. 7-2 was taken at a temperature of 20°C. and a barometric pressure of 742 mm Hg.

The air density (ρ) is defined as, $\rho = \frac{p}{gRT}$ (III-2)

[5]J. H. Dwinell, Principles of Aerodynamics, pp. 25-26, 51-52, McGraw-Hill Co., 1949

where, p = absolute pressure $(\frac{lbs}{ft^2})$

$g = 32.2 \frac{ft}{sec^2}$, acceleration due to gravity

$R = 53.3 \frac{ft}{^oR}$, gas constant

T = absolute temperature (^oR) .

The temperature of 28°C is equal to an absolute temperature of 541.9°R. A pressure of 742 mm Hg. is equal to 2075 lbs/ft^2 at 28°C. Substituting these constants into equation (III-2) gives,

$$\rho = .002235 \text{ lb-sec}^2/\text{ft}^4.$$

Solving for q in terms of V_w and substituting into equation (III-1) gives,

$$T_e = 201.9 \, C_{mg} \, V_w^2 \text{ ft-lbs} . \qquad \text{(III-3)}$$

Equation (3-18) of Section 3 shows the relationship between the error signal (X) and the external load torque (T_e) with respect to the position output angle (Θ_1) of the hydraulic motor. Fig. 3-2 shows the hydraulic system configuration. Thus, the actual input to the hydraulic function (G_h) of Fig. 3-2 for an applied external wind torque is the sum of the error signal (X) and some function of external torque. The hydraulic motor output angle (Θ_1) can then be written as,

$$\Theta_1 = G_h X + G_1 G_h T_e \qquad \text{(III-4)}$$

where G_1 is some transfer function which carries external torque into an error position to be applied to the hydraulic transfer function (G_h). Letting X in equation (III-4) be equal to zero, then $\Theta_1 = G_1 G_h T_e$. (III-5)

Substituting X equal to zero into equation (3-18) gives,

$$\frac{\Theta_1}{T_e} = \frac{(-)\ K_L\ (L+\frac{V}{B}s)}{dm\ N(J_L s^2+f_L s+K_L)\left[dm\ s+(L+\frac{V}{B}s)\frac{J_m}{dm}s^2+(L+\frac{V}{B}s)\frac{K_L}{dm\,N^2}\frac{(J_L s^2+f_L s)}{(J_L s^2+f_L s+K_L)}\right]} \qquad \text{(III-6)}$$

Substituting equation (III-6) into (III-5) gives,

$$G_1 G_h = \frac{(-)\ K_L\ (L+\frac{V}{B}s)}{s\left[dm^2\ N(J_L s^2+f_L s+K_L)+(L+\frac{V}{B}s)NJ_m s(J_L s^2+f_L s+K_L)+(L+\frac{V}{B}s)\frac{K_L}{N}(J_L s+f_L)\right]} \qquad \text{(III-7)}$$

Making the same assumptions as in Section 3, that is, K_L is very large and $\frac{f_L}{N^2(J_m+J_L)} = 0$, equation (III-7) simplifies to,

$$G_1 G_h = \frac{(-)\ (L+\frac{V}{B}s)NB/V(N^2 J_m+J_L)}{s\left[s^2+\frac{BL}{V}s+\frac{B\ dm^2N^2}{V(N^2J_m+J_L)}\right]} \quad . \qquad \text{(III-8)}$$

Dividing equation (III-8) by G_h as given in equation (3-21) gives,

$$G_1 = \frac{(G_1 G_h)}{G_h} = \frac{-(L+\frac{V}{B}s)}{NK_v\ dm} \quad . \qquad \text{(III-9)}$$

Fig. III-1 shows the final block diagram of the hydraulic system with the added complex zero compensation (G_o) and tachometer feedback (G_f) described in Section 4. In addition, the application of T_e through the synthetic transfer function G_1 is represented.

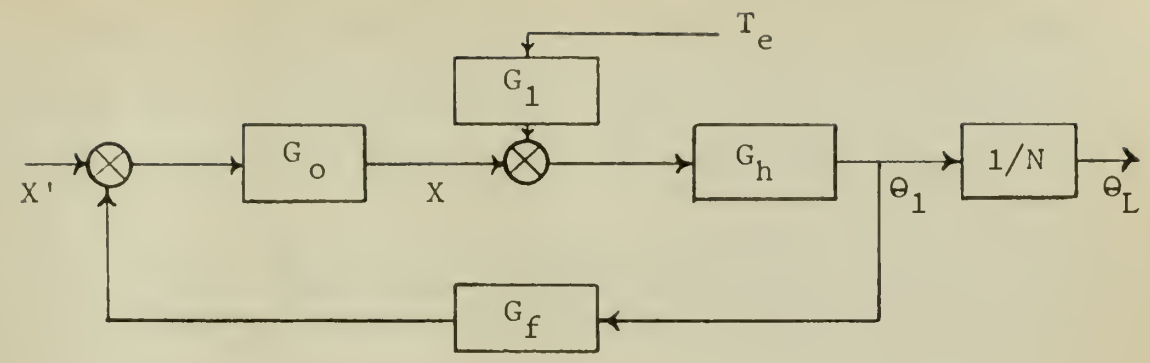

Figure III-1. Block diagram of final hydraulic system.

Assuming that Θ_1 is due to the external torque alone, (ie. X' = O), then

$$\frac{\Theta_L}{T_e} = \frac{G_1 G_h}{N(1 + G_f G_o G_h)} \quad , \qquad \text{(III-10)}$$

where, $G_f = K_f s$, the tachometer feedback

$G_o = K_o$ x (complex roots of G_h), the complex zero compensator added in Section 4.

Substituting equation (III-8) into (III-10) and simplifying gives,

$$\frac{\Theta_L}{T_e} = \frac{(s+BL/V) \;/\; (N^2 J_m + J_L)}{s\left[s^2 + BL/Vs + \dfrac{B\ dm^2\ N^2}{V(N^2 J_m + J_L)}\right]\left[1 + \dfrac{K_f K_o K_v B N^2\ dm}{V(J_L + N^2 J_m)}\right]} \; . \qquad \text{(III-11)}$$

Substituting the hydraulic flow coefficients listed in Section 3 and the gain constants developed in Section 4 into equation (III-11) gives,

$$\frac{\Theta_L}{T_e} = \frac{1.51 \times 10^{-8}(s+42)}{s(s^2+42s+3228)} \quad \text{rad/lb-in} \; . \qquad \text{(III-12)}$$

Combining equations (III-12) and (III-3) enables the solution of the output position angle of the antenna for any given wind velocity. Thus, for a constant C_{mg} ,

$$\frac{\Theta_L}{Vw^2} = \frac{201.9\ C_{mg} \times 1.51\times10^{-8}(s+42)}{s(s^2 + 42s + 3228)} \quad . \qquad \text{(III-13)}$$

APPENDIX IV

ANALOG SIMULATION OF CONDITIONAL FEEDBACK COMPENSATED SYSTEM

Fig. 5-2 shows the block diagram of the complete compensated system under study. It has been shown that only the response of the system to a disturbance input is of interest since the response to the tracking input (R) is known to remain unchanged with the addition of the conditional feedback compensation. Fig. IV-1 shows the block diagram of the compensated system with the tracking input equal to zero.

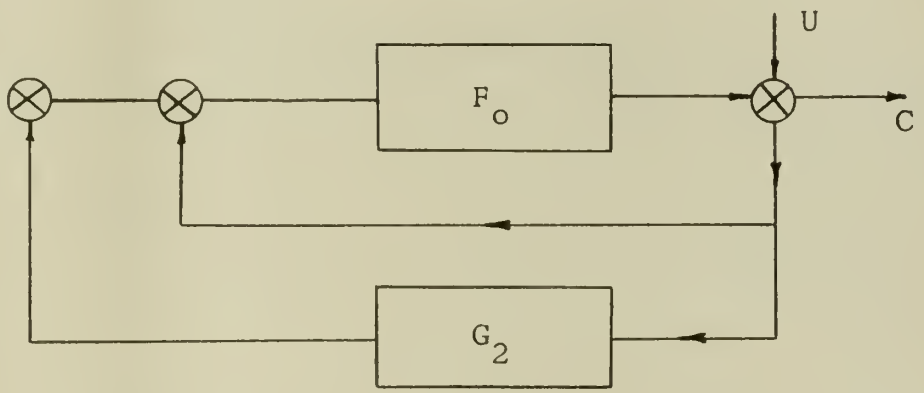

Figure IV-1. System with conditional feedback and R = 0.

The transfer blocks of Fig. IV-1 were defined as follows in Section 4:

$$F_o = \frac{37(s + 1.7)(s + 20)}{s^2 (s + 10)}$$

$$G_2 = \frac{21.06(s + 96)(s + 200)}{(s + 20)(s + 1000)} ,$$

and where U is the disturbance input, (Θ_L), the antenna position due to an applied wind velocity. Equation (III-13) has shown the transfer function from wind velocity (V_w) to

Θ_L to be,

$$\frac{U}{V_w^2} = \frac{\Theta_L}{V_w^2} = \frac{201.9\ C_{mg} \times 1.51 \times 10^{-8}(s + 42)}{s(s^2 + 42s + 3228)}$$

The analog simulation of the compensated system of Fig. IV-1 was undertaken in order to determine the effects of the added conditional feedback compensation on the system response to a simulated wind velocity disturbance profile.

The following is a list of equipment utilized in the simulation of the compensated system:

3- Donner analog computers, Mod. 3000, 10 channels per computer.

1- Brush dual-channel D.C. amplifier.

1- Brush dual-channel pen recorder, Mod. BL-202.

1- Donner variable-base function generator, Mod. 3750.

1- Donner electronic function multiplier, Mod. 3730.

1- Donner null voltmeter, Mod. 5002.

1- Hewlett Packard low frequency function generator, Mod. 202A.

1- Moseley Autograph x-y recorder, Mod. 2-S.

The simulation of the disturbance input function was undertaken in two parts. First, the disturbance torque (T_e) was simulated using equation (III-3),

$$T_e = 201.9\ C_{mg}\ V_w^2 \quad \text{ft-lbs}$$

The representative wind velocity profile of Fig. 7-1 was simulated as a function of time using a variable-base function generator. The simulated profile was generated using

a step velocity input as a time base and an eleven straight-line segment approximation of the wind velocity profile. The constant initial velocity of 25 MPH was then added to the output of the function generator. The resultant was the simulated profile of Fig. 7-1. This velocity profile was squared using the function multiplier. Since C_{mg} was considered constant during the interval of the gust, the squared velocity was multiplied by the appropriate constant to give T_e.

Equation (III-12) gives the transfer function between T_e and the output position due to wind loading (Θ_L). The analog simulation of this transfer function requires an integrating output stage. This equation represents an open-loop transfer function. Therefore, there is no feedback loop around this output stage. Since the input to this integrator is non-zero, this integrating stage would saturate. The simulation was modified to include this integrating stage within the feedback loop of the servo system, resulting in an output from the disturbance simulator of the velocity ($\dot{\Theta}_L$). Modifying equation (III-12) gives,

$$\frac{\dot{U}}{T_e} = \frac{\dot{\Theta}_L}{T_e} = \frac{K_e\ (s + 42)}{(s^2 + 42s + 3228)} \quad ,$$

where K_e is equal to 1.51×10^{-8}.

The velocity $\dot{\Theta}_L$ was added to the velocity output of the transfer function F_o and integrated to obtain the system position output (C).

Fig. IV-2 shows the complete schematic of the analog

computer simulation used. Values of components used as well as the primary outputs are indicated on the figure.

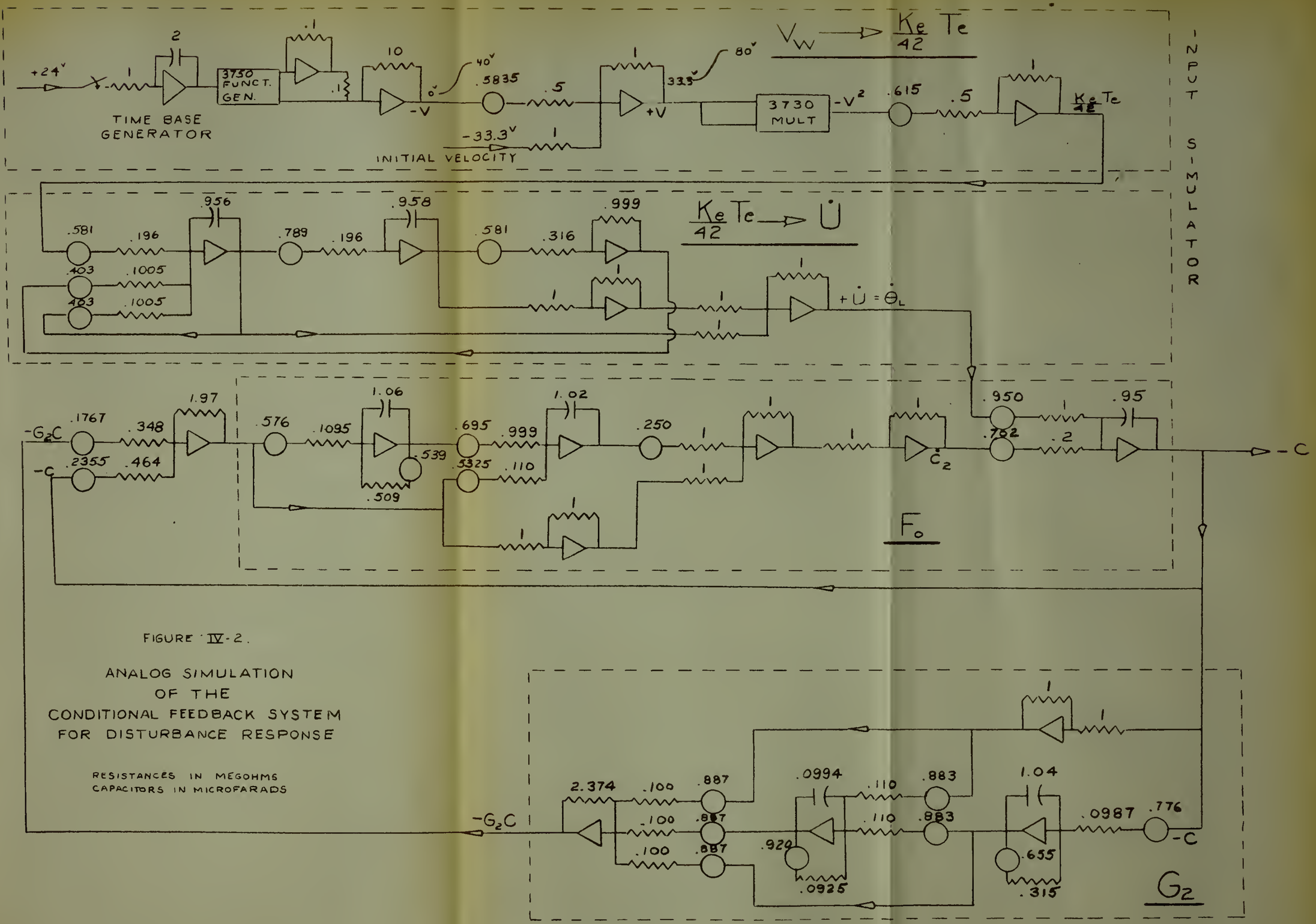

FIGURE IV-2.

ANALOG SIMULATION
OF THE
CONDITIONAL FEEDBACK SYSTEM
FOR DISTURBANCE RESPONSE

RESISTANCES IN MEGOHMS
CAPACITORS IN MICROFARADS